Doctoral Dissertation

Engineering of orthogonal synapse organizers for multiplexed cell-specific interface between neurons and microelectrodes

LI JIALIN

Supervisor：Tsutsui Hidekazu

Division of Advanced Science and Technology

Japan Advanced Institute of Science and Technology

[Materials Science]

December 2025

Table of Content

Abstract

Neuronal circuits are complex networks composed of diverse types of neurons that provide the functional flexibility of living organisms. It is generally thought that each type of neuron plays a distinct role, and together they enable the integrated operation of the entire circuit. Therefore, techniques that selectively record the activity of specific neuronal types are indispensable for studies of neural circuits. Microelectrode technique has long been one of the major methods for recording neural activity with millisecond precision. However, because it lacks cell-type specificity, identifying neuronal types requires the use of cumbersome and indirect auxiliary methods. This limitation becomes even more critical in recently developed multi-electrode array technologies, where distinguishing neuronal types has become increasingly difficult.

To confer cellular selectivity on electrodes, this study set out to engineer an orthogonal library of synapse organizers functioning as molecular “lock-and-key” switches. These tools were designed so that a receptor-functionalized microelectrode could induce the formation of presynapse-like structures on axons expressing the corresponding ligand-tagged organizer, in a cell-type-specific manner. The study also sought to determine the ligand–receptor affinities required for such tools.

Three polycistronic constructs—Spot-, V5-, and Alfa-cNrxn1βΔECD—were generated, each fused via a P2A peptide to EGFP-Rab3 as a fluorescent presynaptic marker. Truncation of the LNS domain eliminated binding to endogenous neuroligins, ensuring that synapse induction was strictly dependent on ligand–nanobody interactions. Reported affinities of the peptide–nanobody pairs span from 26 pM (Alfa) to 29 nM (V5). HEK293T surface-display assays confirmed strict one-to-one recognition: only the

cognate nanobody produced robust membrane fluorescence, even under saturating ligand concentrations (up to 8 μM). Primary chick forebrain neurons were transfected with the constructs and cultured overnight with nanobody-decorated microbeads. Synapse formation was quantified by EGFP-Rab3 accumulation at axon–bead contacts, and statistical analysis was performed using Kruskal–Wallis followed by Dunn's post-hoc tests. Targeted contacts (e.g., Spot construct + anti-SpotNb beads) showed significantly higher Rab3 indices than any off-target combination. No significant differences were detected among the three on-target pairs, indicating comparable synaptogenic potency despite an ~1000-fold range in dissociation constant (Kd). These results establish Spot, V5, and Alfa tags as a bona fide orthogonal trio well suited for multiplexed interfacing. The molecular tools described here are expected to provide a platform for precise, genetically targeted, and multiplexed electrophysiological recording in future. This dissertation is organized into five main chapters. Chapter 1 serves as a general introduction, outlining the basic concepts of key components discussed in this work, including neurons, synapses, and microelectrode technology. Chapter 2 provides a detailed discussion of the background of synapse organizers and their applications in experiments, representing the central focus of this study. Chapter 3 describes the experimental principles and procedures employed in this research, as well as the methods for data acquisition and analysis. Chapter 4 presents and analyzes the experimental results in detail, drawing the corresponding conclusions. Finally, Chapter 5 summarizes the results and conclusions as a whole and offers perspectives for future studies.

Keywords

Neurons, Neuronal Circuits, Synapses, Synapse Organizers, Microelectrode Technique, Dissociation constant, Orthogonality, Engineered synapse organizers

Objectives

Developing a powerful technique that enables precise measurement of neuronal circuit activity is one of the major challenges for understanding the principles of information coding and processing in neural circuits (G. H. Kim et al., 2018; Roth & Ding, 2020). Extracellular recording is a type of microelectrode-based electrophysiological method that detects voltage fluctuations in the vicinity of neurons (Buzsáki, 2004; J. Zhang et al., 2014). This method generally provides high temporal resolution while maintaining a satisfactory signal-to-noise ratio (K. D. Harris et al., 2016). Furthermore, advances in flexible array electrodes have made it possible to perform large-scale parallel recordings from deep tissue (Buzsáki, 2004; Hong & Lieber, 2019) . Thus, this microelectrode technique has become one of the major experimental approaches for elucidating the mechanisms of information coding and processing in neural circuits (G. H. Kim et al., 2018). However, it suffers from a critical limitation: it inherently lacks specificity for particular cell types (K. D. Harris & Mrsic-Flogel, 2013).

To bridge this gap, synapse-organizing proteins—natural mediators of intercellular adhesion—have been proposed (Südhof,2018). These proteins exhibit robust synaptogenic activity and retain their ability to induce synapse formation even when immobilized on artificial surfaces (Scheiffele et al., 2000). Previous studies demonstrated that chimeric neurexin-1β (cNrxn1βΔECD), fused to a peptide ligand (Spot-tag), enabled presynaptic differentiation of contacting axons when presented on gold electrodes

functionalized with anti-Spot nanobodies (Nb) (Hamid et al., 2023). This work established the concept of a molecularly inducible neuron–electrode interface (Fig. 1a).

Recent advances in single-cell transcriptomics have revealed the extraordinary diversity of neurons constituting neural circuits (Xing et al., 2023). One of the latest analyses reports that mouse neurons can be classified into more than 5,000 clusters (M. Zhang et al., 2023). It is thought that the integrative function of neural circuits arises from the distinct contributions of these different cell types (Economo et al., 2024). Therefore, to probe such circuit functions, orthogonal molecular tools for inducing synaptic differentiation are required. Here, “orthogonal” molecular tools refer to multiple sets of molecules that do not cross-react or interfere with one another.

This study has two main objectives. The first is to demonstrate, as a proof of principle, whether it is feasible to design molecular tools with true orthogonality. The second is to clarify the range of ligand–receptor affinity required for engineered synapse organizers. To achieve these goals, this study employs three peptide tags—Spot, Alfa, and V5—as ligands. For each of these, a nanobody with highly specific binding has been developed, and the reported dissociation constants (K_d) span nearly three orders of magnitude, from 26 pM to 29 nM (Braun et al., 2016; Götzke et al., 2019; Virant et al., 2018; Zeghal et al., 2023). Thus, these ligand–receptor pairs were considered optimal for investigating the affinity requirements of engineered synapse organizers.

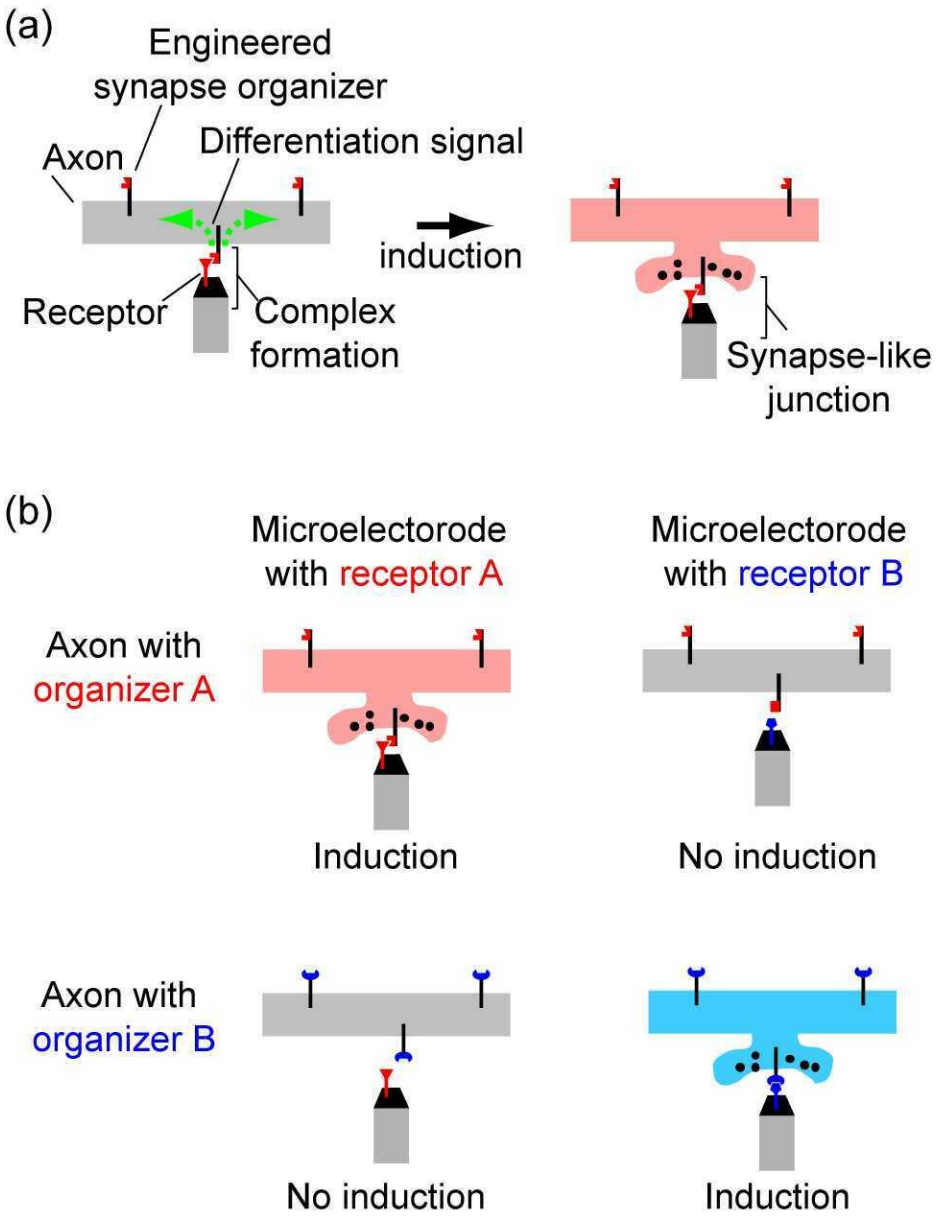

Fig. 1. (a) Concept of the molecularly inducible neuron-microelectrode junction.

(b) Concept of an orthogonal set of engineered synapse organizers.

Chapter 1

General Introduction

The following is a description of the terms used in this paper, such as cell biology, electrophysiology, and molecular biology.

1.1 Neurons

Neuron is the basic structure and functional unit of nervous system, which is responsible for receiving, integrating and transmitting information (Bigbee, 2023). Its main structure consists of Cell body, Dendrites, Axon and Synaptic Termina. Neurons consist of a cell body and two types of cytoplasmic processes that extend from the cell body. One of these structures, the axon, transmits information to other neurons and muscles, while the other structure, the dendrite, receives information from other neurons. There is usually one axon per neuron, and multiple dendrites. Neurons have two main functions: electrical signal conduction and information integration. It generates action potential through sodium/potassium ion channel (for example, the transmission speed of tactile signal can reach 120 m/s). Neurons can receive hundreds of input signals in dendrites, and cell bodies decide whether to trigger action potentials (Ludwig et al., 2025).

1.2 Synapses

Synapse is a functional connection point between neurons or between neurons and effector cells (such as muscles and glands), which is responsible for the chemical or electrical transmission of signals. The structure consists of synapses are presynaptic membrane, synaptic cleft and postsynaptic membrane. Synapse is a “transfer station” of information, which can be precisely regulated by chemical signals Fig.2 (Gentile et al., 2022).

The two work together to build a dynamic neural network, which supports all life activities from breathing to thinking. Studying the mechanism of neurons and synapses is the core of understanding brain function, developing AI algorithm and treating neurological diseases. Neurons are like the CPU of a computer, and synapses are circuit board nodes connecting the CPU, which together form a powerful “biological computer”.

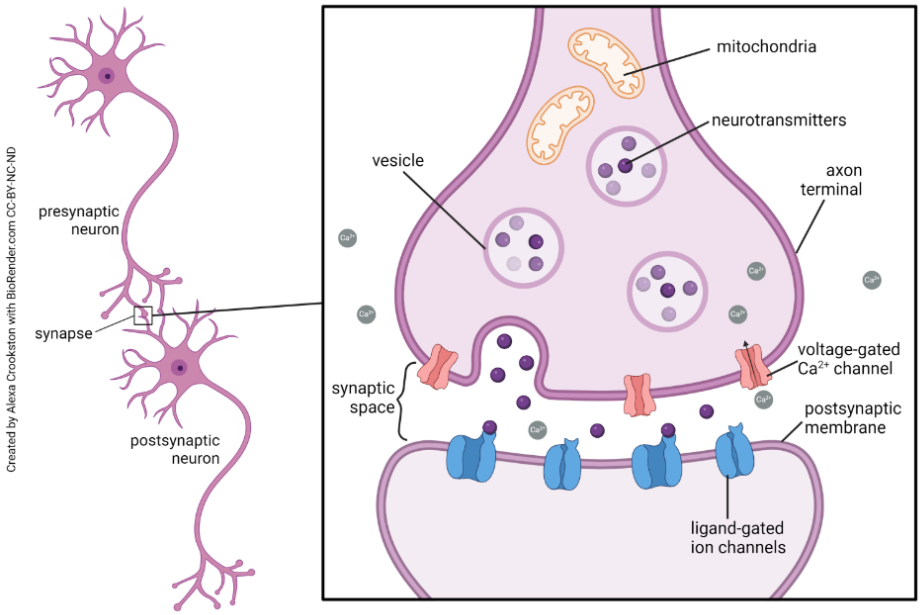

Fig. 2. Synapse structure (Jim Hutchins, Travis Price, et al., Integrated Human Anatomy and Phsiology Part 2).

1.3 Synapse organizer

Synapse organizer is a kind of molecule that mediates the formation, maintenance and functional regulation of synapses, and accurately guides the structural assembly and signal transmission of presynaptic membranes and postsynaptic membranes through the interaction of transmembrane or secretory proteins (Connor & Siddiqui, 2023).

Its core functions include determining the position and specificity of synapses and regulating synaptic transmission efficiency. Synapse organizers maintaining excitatory/inhibitory synaptic balance, and they are known to induce synaptic differentiation (Molecular Structure and Engineering of Synaptic Organizer Proteins in Health and Disease, 2020).

1.4 Types of synapse organizers

Synapse organizers are trans-synaptic adhesion proteins that dictate where, when, and what type of synapses form. The best-known family is Neurexin–Neuroligin, which exists in α- and β-isoforms and splices into excitatory (NLGN1/3) or inhibitory (NLGN2) (Stokes et al., 2024; Südhof, 2008; Xue et al., 2022). In the cerebellum, Cbln1 secreted from climbing fibers binds GluD2 on Purkinje cells (Kd ≈ 180 nM) to establish parallel-fiber synapses (Ichtchenko et al., 1995). LRRTMs (leucine-rich repeat transmembrane proteins) selectively pair with neurexins to promote excitatory synapses. IL1RAPL1–PTPσ complexes drive inhibitory synapse formation and are linked to X-linked intellectual disability. Nectin-3-Afadin tethers synapses to adherent junctions for precise subcellular positioning (Ko et al., 2009). Emerging members include Teneurins, Dystroglycan, and Ephrin/Eph systems, each offering unique affinity ranges and downstream signaling motifs. These organizers collectively ensure cell-type specificity, circuit balance, and synaptic plasticity across the nervous system.

1.5 Neurexin and Neuroligin

Neurexins and neuroligins are the archetypal synapse organizers. Neurexins are presynaptic, polymorphic cell-surface proteins generated from three genes (NRXN1-3) via α- and β-splice isoforms, while neuroligins (NLGN1-4) are postsynaptic adhesion molecules. Their Ca^{2+}-dependent heterophilic interaction bridges the synaptic cleft (Ichtchenko et al., 1995; Südhof, 2008), clustering vesicles on the presynaptic side and recruiting NMDA/AMPA or GABA_A receptors. Alternative splicing of neurexins and cell-type expression of neuroligin isoforms confer excitatory versus inhibitory synapse identity. Structural studies reveal how glycosylation and splice inserts modulate binding strength, making the pair a tunable scaffold for neural circuit assembly (Ichtchenko et al., 1995).

1.6 Neuron Circuit

A neural circuit is a network of interconnected neurons that process and transmit information through electrical and chemical signals. It consists of excitatory (glutamatergic) , inhibitory (GABAergic), and modulatory (dopaminergic, serotonergic) cells working in precise balance. Inputs from sensory or other brain regions trigger action potentials, causing neurotransmitter release at synapses. The circuit integrates, filters, and stores information, enabling perception, decision-making, and motor control (Yau et al. 2015).

1.7 Microelectrode Technique

membrane voltage optical imaging Extracellular recording (Bando et al., 2019; Tsutsui et al., 2008, 2013), a subset of this technique, involves placing microelectrodes near cells to detect voltage changes without penetrating the cell membrane（Hubel & Wiesel, 1959; Jun et al., 2017）. This method is widely used due to its minimal invasiveness and ability to record activity over extended periods (Obien et al., 2015; Tsutsui et al., 2013).

Microelectrodes, typically made of metal (e.g., tungsten, platinum) or glass pipettes filled with electrolytes, have micrometer-scale tips. In extracellular recording, the electrode is positioned adjacent to a neuron. When the neuron fires an action potential, ion fluxes (e.g., Na^+, K^+) generate extracellular currents, which the electrode detects as voltage fluctuations. These signals are smaller in amplitude (microvolts to millivolts) compared to intracellular recordings and may include activity from multiple neurons (Xu et al., 2025).

We applied Patch clamp technique in our research. Patch clamp or multi-electrode array records the electrical activity of neurons and reveals the loop dynamics. It is a powerful electrophysiological technique that can directly measure membrane potential and the amount of current passing through the cell membrane, and is still a standard technique in electrophysiology and neuroscience (Hamill et al., 1981).

Chapter 2

Synapse Organizer Background

2.1 Introduction

Synapses are the fundamental connections for communication between neurons in the nervous system, consisting of presynaptic terminals (axons) and postsynaptic membranes (dendrites or cell bodies). The formation, maintenance, and specificity of these synapses are controlled by synaptic organizers, who are crucial for assembling the presynaptic and postsynaptic structures required for neurotransmitter release and reception (Gentile et al., 2022).

The research on synaptic organizers has great potential in addressing biological electronic interfaces, especially in achieving cell type specific recording of neural activity. Traditional electrophysiological techniques, such as patch clamp and microelectrode array, lack inherent selectivity for specific neurons, thus requiring indirect methods such as genetic markers or waveform analysis (K. D. Harris & Mrsic-Flogel, 2013). By utilizing synaptic organizers, researchers can design molecularly induced neuronal microelectrode interfaces that can selectively target and record gene defined neurons.

2.2 The stage of synapse formation

1. Differentiation and Migration of Neurons

In the early stages of nervous system development, neurons differentiate from neural stem cells. Neural stem cells have multi-directional differentiation potential and can differentiate into various types of nerve cells such as neurons, astrocytes, and oligodendrocytes. During the differentiation process, neural stem cells first undergo a proliferation stage and then differentiate into neuronal precursor cells under specific

signal induction. These precursor cells further differentiate into mature neurons and begin to migrate to their final functional sites.

2. Growth of axons and dendrites

After neuronal differentiation, its axons and dendrites begin to grow. Axons are the output parts of neurons, responsible for transmitting signals to other neurons or effector cells; Dendrites are input components that receive signals from other neurons. The growth of axons and dendrites is the basis for establishing functional connections in neurons, and this process is regulated by various growth factors and extracellular signals.

3. Pre synaptic and Post synaptic Differentiation

When axons and dendrites grow and come into contact with each other, presynaptic and postsynaptic differentiation begins. Presynaptic differentiation refers to the formation of a presynaptic membrane at the end of axons, which can store and release neurotransmitters; Post synaptic differentiation refers to the formation of a postsynaptic membrane in dendrites or cell bodies, which can receive neurotransmitters and produce electrophysiological responses. This process is a crucial step in synapse formation, involving multiple synapse organizers and intracellular signaling pathways.

4. Maturity and functionalization of synapses

After synapse formation, further maturation is required to achieve effective neural signal transmission. This includes the refinement of presynaptic neurotransmitter release mechanisms, the aggregation and functionalization of postsynaptic receptors, and the stabilization of synaptic structures. The maturation of synapses is a dynamic process that

is regulated by multiple factors, including neural activity, neurotrophic factors, and intracellular signaling pathways.

In summary, the formation of synapses is a complex and orderly process that involves multiple stages and molecular mechanisms. From the differentiation and migration of neurons to the maturation and functionalization of synapses, every stage is precisely regulated. Therefore, in-depth study of the mechanism of synaptic formation not only helps us understand the normal function of the nervous system, but also provides an important theoretical basis for the diagnosis and treatment of related diseases (Martin et al., 2021).

2.3 Molecular Mechanisms of Synapse Organizers

1. The role of synaptic organizers

Synaptic organizers are a critical class of membrane proteins that form complexes on the presynaptic and postsynaptic cell membranes, promoting synapse formation and differentiation through interactions. These proteins play a crucial role in the specific formation and functionalization of synapses, ensuring precise and effective connections between neurons (Connor and Siddiqui 2023).

2. Intracellular signaling pathways

The interaction between synaptic organizers activates various intracellular signaling pathways, which play a crucial role in synaptic formation and functionalization. These signaling pathways ensure the normal development and function of synapses by regulating protein synthesis, transport, localization, and function（K. P. Harris & Littleton,

2015).

For example, the PI3K Akt mTOR signaling pathway plays an important role in the synthesis and transport of synaptic proteins. After activation of PI3K (phosphatidylinositol 3-kinase), Akt (protein kinase B) can be phosphorylated, thereby activating mTOR (mammalian target protein of rapamycin). MTOR is a crucial nutrient and energy sensor within cells, which promotes the synthesis and transport of synaptic proteins by regulating protein synthesis and cell growth (Kommaddi et al., 2024). The activation of this pathway is crucial for the maturation of presynaptic and postsynaptic structures.

3. The regulatory role of neural activity

Neural activity plays an important regulatory role in the formation and functionalization of synapses. Through the mechanism of neural activity dependence, synapses can be adjusted and optimized based on the activity level of neurons. This activity relies on regulatory mechanisms that form the basis of neural plasticity, enabling the nervous system to adjust its structure and function based on experience or learning.

For example, long-term potentiation (LTP) and long-term depression (LTD) are two typical synaptic plasticity phenomena that depend on neural activity. LTP refers to the phenomenon where the strength and function of synapses are enhanced under high-frequency stimulation; LTD is a phenomenon in which the strength and function of synapses weaken under low-frequency stimulation (Anjum et al., 2024). These two phenomena optimize the connections of neural networks by altering the structure and function of synapses.

The formation and functionalization of synapses is a complex and intricate process involving multiple molecular mechanisms and cellular signaling pathways. Synaptic organizers activate intracellular signaling pathways through interactions, promoting the formation and differentiation of synapses. These signaling pathways not only regulate the synthesis and transport of synaptic proteins, but also participate in the remodeling and stabilization of synaptic structures. In addition, neural activity further optimizes synaptic function through activity dependent mechanisms such as LTP and LTD, enabling the nervous system to dynamically adjust based on experience or learning.

2.4 Dissociation constant of nature synapse organizer

The dissociation constant (Kd) usually quantifies how tightly a synapse-organizing protein binds to its natural partner. Kd values allow researchers to rank how strongly different neurexin–ligand pairs stabilize synapses. For example, neurexin-1β binds NL-1 with ~30 nM affinity—comparable to high-affinity antibody–antigen interactions—explaining why NL-1 overexpression rapidly induces presynaptic differentiation. Knowing the native Kd helps design artificial organizers whose ligand–nanobody affinity can be tuned to avoid or mimic natural interactions.

Accurate Kd measurements (via SPR, ITC, or Scatchard) ensure that in vitro assays (microbeads, microelectrodes) use ligand concentrations in the correct stoichiometric window, preventing false-negative or artefactual results. In short, Kd tells us whether the binding between molecules is strong or weak each time, which is the basis for evaluating the feasibility of synaptic biology to neural interface engineering.

2.5 Role of Synapse Organizers in Bioelectronics

Synaptic organizers play a crucial role in bioelectronics, particularly in the development of cell type specific neural microelectrode interfaces.

Specific synaptic organizers form complexes in axons and dendrites, which trigger cellular signaling when they come into contact, leading to differentiation into presynaptic and postsynaptic compartments. When the surface of microelectrodes is modified by receptors of synaptic organizers and comes into contact with target neurons expressing these organizers, they can send differentiation signals, forming synaptic like neural microelectrode connections. By utilizing the function of synaptic organizers, highly specific neural interfaces can be developed, which is of great significance for neural repair and brain computer interfaces in the field of bioelectronics. For example, gold microelectrodes modified with interleukin-1 receptor helper protein like 1 (IL1RAPL1) can send differentiation signals to cortical neurons upon contact (Montani et al., 2019). This specific connection helps improve the accuracy and efficiency of neural signal recording and stimulation.

In summary, synaptic organizers provide new strategies and tools for the development of neural microelectrode interfaces in bioelectronics, contributing to more precise and efficient neural interface technologies.

2.6 Advantages of Engineered Synapse Organizers

1. Cell type specificity

Engineering synaptic organizers can be designed specifically for certain types of neurons. This specificity is crucial for applications such as brain computer interfaces (BCIs) and neural prostheses (Yao et al., 2023), where precise connections are required to achieve optimal functionality (Serruya et al., 2018). By targeting specific cell types, these organizers minimize the risk of accidental connections with other neurons, reduce noise, and improve the signal-to-noise ratio in neural recordings.

2. Enhance stability and robustness

Engineering organizers can establish stable and persistent connections between neurons and microelectrodes. This stability is crucial for the chronic implantation and long-term monitoring of medical devices (Suzuki et al., 2020). These organizers are able to maintain their functions even under different environmental conditions, such as changes in temperature, pH, and mechanical stress, which are common in biological environments.

3. Rapid formation of synapses

Compared to natural processes, engineered synaptic organizers can induce synaptic formation faster. For example, some engineering organizers can trigger synaptic differentiation within hours, significantly accelerating this process compared to natural synapse formation. This rapid formation allows for faster integration of neural interfaces, which is particularly beneficial in clinical environments where time is a critical factor.

4. Customizability

Engineers can customize organizers to suit specific applications. For example, they can modify the organizer to interact with specific receptors or function under specific conditions. This customizability extends to different types of neural interfaces, from microelectrode arrays to optogenetic devices, making engineering synaptic organizers a multifunctional tool in bioelectronics.

5. Research and development potential

Engineering synapse organizers provide powerful tools for researchers to study synapse formation, neural connections, and neurodegenerative diseases. They have opened up new avenues for innovation in bioelectronics, encouraging the development of next-generation neural interfaces and therapies.

In summary, the advantages of engineering synaptic organizers in these areas make them promising technologies for advancing the field of bioelectronics and improving neural interface performance.

2.7 Previous experimental applications

In previous studies conducted in our laboratory, researchers genetically engineered neurexin-1β to eliminate its natural receptor-binding domain (LNS domain) to prevent interaction with endogenous molecules. They then inserted exogenous ligands (such as Spot-tag, FLAG, or YFP-null) to facilitate artificial clustering mediated by antibodies/nanobodies (such as anti-SpotNb) (Sekine et al., 2024).

Design Strategy for Previous Research

Component	Native Neurexin-1β	Engineered Organizer
Extracellular Domain	LNS (binds Nlgn1)	Replaced with exogenous ligands (e.g., Spot-tag, YFP-null)
Downstream Marker	None	P2A peptide co-expressing EGFP-Rab3 (presynaptic marker)
Targeting Receptor	Neuroligin-1	Nanobodies (e.g., anti-SpotNb, anti-FLAG)

The researchers conducted a verification experiment: after expressing artificial organizers in neurons, antibody-modified microbeads were used to induce the aggregation of presynaptic markers (such as EGFP-Rab3) (Haga et al. 2024; Sekine et al. 2024). The receptor of the artificial organizer (anti-SpotNb) was immobilized on a gold microelectrode, confirming that it could specifically induce the formation of synaptic-like connections in neurons expressing the organizer .

Researchers discovered a functional decoupling between the extracellular binding domain (LNS) and the intracellular signaling domain of neurexin-1β. Neurexin-1β lacking the LNS domain (ΔECD1/2) can still induce presynaptic differentiation through clustering mediated by antibodies or nanobodies.

This series of studies provides a theoretical basis for artificial modification – activating downstream signaling without the need for natural ligand binding, solely through physical clustering.

2.8 Challenges and Future Directions

1. Function Verification

Neurotransmission: One of the main challenges is to ensure that induced synapses exhibit normal neural transmission. This involves verifying whether synaptic vesicles respond to electrical signals to release neurotransmitters, and whether these neurotransmitters effectively bind to receptors on postsynaptic neurons, thereby triggering appropriate electrical responses. Techniques such as electrophysiological recording and fluorescence imaging of neurotransmitter release can be used to verify this function.

Long term stability: The durability of electrode neuron connections over a long period of time (several days to several weeks) is crucial for practical applications. This stability is influenced by factors such as the biocompatibility of electrode materials, the robustness of synaptic connections, and the system's ability to withstand the dynamic environment of living tissues. Long term research is necessary to evaluate the performance and integrity of these connections under various physiological conditions.

2. Optimization

Electrode optimization: Optimizing electrode design to achieve optimal balance requires consideration of factors such as electrode size, shape, and material composition. Advanced materials and nanomanufacturing technologies can be explored to enhance these properties.

Protein immobilization: Improving the efficiency of synaptic organizer attachment to electrode surfaces is another key optimization area. This involves developing methods to ensure that synaptic organizers are securely and uniformly fixed on the electrode surface

without affecting their biological activity. The chemical functionalization of electrode surfaces, the use of connecting molecules, and the optimization of fixation conditions can improve the adhesion efficiency and stability of organizers.

3. Extension to other organizers

Other synaptic organizers: Although Neurexin-1 β (NRXN-1 β) has been widely studied and utilized, it is necessary to explore other synaptic organizers for broader applications. For example, the IL1RAPL-PTP δ complex and leucine rich repetitive transmembrane proteins (LRRTMs) are promising candidates. Designing these organizers can provide additional functionality to improve the specificity and efficiency of synaptic connections.

Diversified applications: Expanding the scope of synaptic organizers can open up new avenues for the application of various neural interfaces. For example, different organizers may be more suitable for specific types of neurons or neural circuits, thereby achieving more targeted and effective interfaces in different regions of the brain or nervous system.

4. Impact on Neuroscience and Medicine

Targeted recording: The ability to achieve targeted recording from genetically defined neurons in disease models brings great hope for advancing our understanding of neurological diseases. By selectively connecting with these neurons using engineered synaptic organizers, researchers can gain detailed insights into the neural activity patterns and circuit dysfunction associated with these diseases. This can lead to the development of more effective diagnostic tools and treatment strategies.

Therapeutic equipment: The development of implantable electrodes for closed-loop neural regulation of neurological diseases is another exciting application. A closed-loop

system can provide real-time monitoring and stimulation, allowing for precise and adaptive regulation of neural activity. For example, in epilepsy, such devices can detect epileptic activity and provide targeted electrical stimulation to prevent or alleviate seizures. The use of engineered synaptic organizers can improve the specificity and efficacy of these therapeutic devices.

Chapter 3

Methodological Principles

3.1 PCR based molecular cloning and purification from plasmid DNA amplification

3.1.1 Primer design

Primer design is the most important factor in insert-making for the desired vector plasmid. This primer design is crucial for successful synapse organizer making. Primers designed for the PCR were about 500 to 900 base pairs (bp) in total. Inserts were the same lengths with restriction enzymes as in the plasmid vector digestion sites. Firstly, input the targeted bp genomic DNA sequences into the online NCBI primer BLAST software, then about 18-22 bp nucleotide sequences were selected as a primer to amplify 500-900 bp for inserts, then made reverse primer then I added the restriction enzymes in both forward and reverse primer. During the design of the primer, some factors like the percentage of GC content, melting temperature, and self-complementary should be considered.

3.1.2 PCR Amplification

PCR amplification was started after making the following dilution:

Pure water	10µl
Prime Star Max enzyme	10µl
Primer Forward	0.2µl
Primer Reverse	0.2µl
Template diluted (1:100)	1µl
Total	21.4µl

For Template, miniprep should be 100-time dilution, the following temperature cycle was

maintained:

Segment	Repeat	Temperature	Time
1	1	95℃	2 minutes
2	30	98℃ 55℃ 72℃	10 seconds 15 seconds 50 seconds
3		72℃	5 minutes
4		4℃	99.99

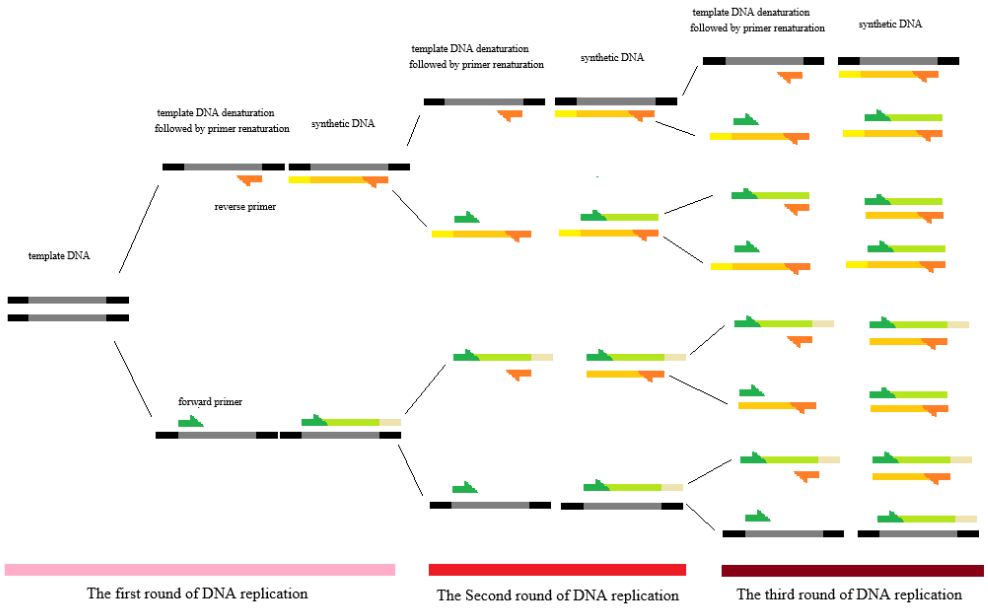

Figure 3: DNA amplification of PCR.

3.1.3 Enzyme Digestion

The vectors and inserts were prepared using restriction enzymes.

The digestion reaction as follows: 2 µl DNA, 3 µl digestion buffer, 25 µl ddH_2O, and 0.5 µL restriction enzyme, for a total volume of 30.5 µl. The reaction mixture was incubated at 37°C for 60 minutes to complete the first digestion.

3.1.4 Agarose Gel Electrophoresis

To prepare the agarose gel, I initially added 0.5 grams of agarose powder to 50 milliliters of 1× TAE buffer. Alternatively, an agarose tablet can be used in place of the powder to achieve the same concentration. The mixture was then heated in a microwave for approximately one and a half minutes, carefully monitoring to ensure the solution became completely clear, indicating that the agarose had fully dissolved. Once the solution reached a clear appearance, it was ready for pouring.

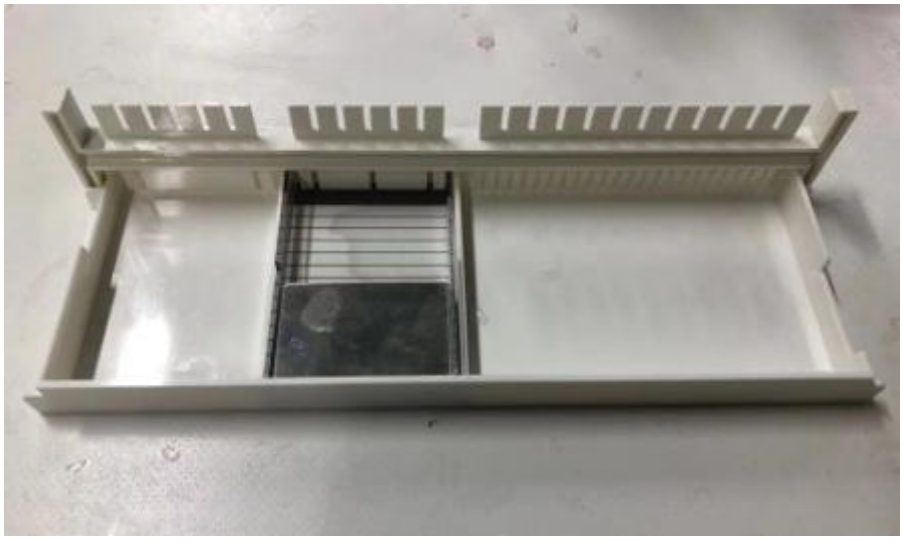

Figure 4 : Cassette with a comb for agarose gel making.

Next, prepare the gel cassettes by inserting the desired comb to create wells. The agarose

solution was carefully poured into the cassette, ensuring an even distribution. The cassette was then left undisturbed for about 30 minutes to allow the gel to solidify. After this period, the comb was carefully removed to avoid damaging the wells, and the solidified gel was placed into the agarose gel electrophoresis chamber.

Before running the electrophoresis, load the wells of the gel with the marker and samples. Specifically, 4 microliters of a 1Kbp DNA ladder were loaded as the marker, followed by the samples mixed with loading buffer into the adjacent wells. The electrophoresis chamber was then connected to a power supply, and a voltage of 100 volts was applied.

The agarose gel electrophoresis was run for approximately 30 minutes to allow the samples and marker to migrate properly through the gel matrix. After this duration, the electrophoresis was halted, and the gel was carefully removed from the chamber and placed into an ethidium bromide staining solution. This staining solution was prepared earlier by mixing 5 microliters of ethidium bromide with 200 milliliters of 1× TAE buffer. The gel was left in the staining solution for about 20 minutes to allow the ethidium bromide to bind to the DNA, making it visible under UV light.

Finally, the stained gel was placed on a UV transilluminator, and the band patterns of the desired DNA inserts were examined. This step allowed for the visualization and verification of the DNA fragments, confirming the successful preparation and separation of the samples.

3.1.5 PCR Gel Clean-Up

To purify PCR products and remove contaminants such as salts, enzymes, and excess reagents (ensuring SDS concentration < 0.1%), the following detailed protocol was meticulously followed:

① Adjust DNA Binding Conditions

For PCR reaction volumes smaller than 30 µl, the total volume was adjusted to 50-100 µl by adding distilled water. If mineral oil was present, it was not necessary to remove it.

The sample was mixed with an equal volume of Buffer NT1. For example, 100 µl of PCR reaction mixture was combined with 200 µl of Buffer NT1 to facilitate optimal binding conditions.

If the sample included dissolved gel fragments, the tube was incubated at 42°C for 5 minutes to ensure complete dissolution.

② Bind DNA

A NucleoSpin® Gel and PCR Clean-up Column was assembled and placed into a 2 ml collection tube.

Up to 700 µl of the prepared sample mixture was carefully loaded onto the column.

The column was centrifuged at 11,000 x g for 30 seconds to bind the DNA to the silica membrane.

The flow-through was discarded, and the column was placed back into the collection tube.

If additional sample volume remained, it was loaded onto the column, and the centrifugation step was repeated.

③ Wash Silica Membrane

700 µl of Buffer NT3 was added to the column to wash away non-specific contaminants. The column was centrifuged at 11,000 x g for 30 seconds. The flow-through was discarded, and the column was placed back into the collection tube. This washing step

was repeated to ensure the removal of chaotropic salts and other impurities.

④ Dry Silica Membrane

The column was centrifuged for an additional 1 minute at 11,000 x g to thoroughly dry the silica membrane and remove any residual Buffer NT3.

Care was taken to avoid contact between the spin column and the flow-through during removal from the centrifuge and collection tube to prevent contamination.

⑤ Elute DNA

The NucleoSpin® Gel and PCR Clean-up Column was transferred to a new 1.5 ml microcentrifuge tube.

15-30 µl of Buffer NE was added directly onto the silica membrane.

The column was incubated at room temperature (18-25°C) for 1 minute to allow the DNA to elute from the membrane.

Finally, the column was centrifuged at 11,000 x g for 1 minute to collect the purified DNA in the microcentrifuge tube.

3.1.6 Ligation and transformation

For the ligation reaction, the mixture was incubated at 16°C for 30 to 60 minutes to allow the DNA fragments to join together efficiently. Following this, 25 µl of the ligation mixture was used to transform competent E. coli (DH5α) cells.

The transformation process involved several precise temperature steps:

1.The transformation mixture was first placed on ice for 10 minutes to cool the cells.

2.It was then transferred to a 42°C water bath for 45 seconds to briefly heat-shock the cells, facilitating the uptake of the plasmid DNA.

3.Immediately after the heat shock, the mixture was returned to ice for another 10 minutes to stabilize the transformed cells.

After the transformation, the E. coli cells were spread onto an agar plate containing ampicillin, depending on the antibiotic resistance of the plasmid. The plate was then incubated overnight at 37°C to allow the transformed cells to grow and form colonies.

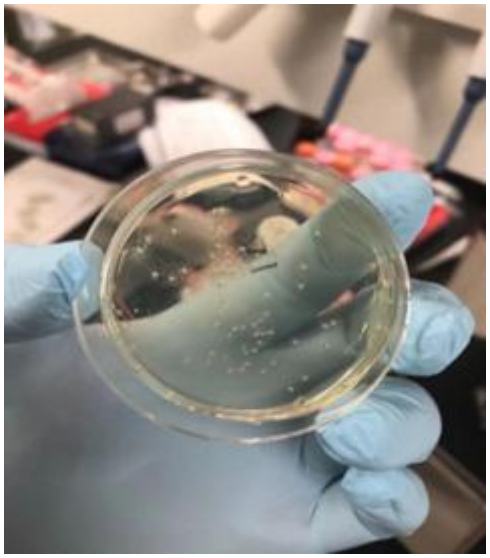

Figure 5 : Colonies found after successful ligation of vector and insert

3.1.7 Miniprep Procedure

To perform the miniprep procedure, pick a single bacterial colony with sterile toothpick from an agar plate and transfer it into a glass tube containing LB medium supplemented with the appropriate antibiotic used in the plate culture. The tube was then incubated overnight at 37°C to allow the bacteria to grow.

The next morning, transfer the bacterial culture into a 2 ml microcentrifuge tube and

centrifuged it at 5000 rpm for 3 minutes to pellet the cells. The supernatant (LB medium) was carefully discarded, as the cells had formed a pellet at the bottom. Add 200 µl of Cell Resuspension Buffer (CRA) to resuspend the cell pellet, followed by 200 µl of Cell Lysis Buffer (CLA). Instead of vortexing, gently mix the contents by inverting the tube several times to avoid creating bubbles or foam, which could shear the DNA.

After allowing the tube to sit for 3 minutes to ensure complete cell lysis, add 5 µl of Alkaline Protease and gently mixed by inverting the tube. The tube was left open at room temperature for another 3 minutes. Next, add 300 µl of Neutralization Solution (NSB) and mix thoroughly by inverting the tube several times. The mixture was then centrifuged at 14000 rpm for 10 minutes to separate the cellular debris.

Prepare a NucleoSpin® Gel and PCR Clean-up Column and pour the supernatant containing the plasmid DNA into the column. The column was centrifuged at 5000 rpm for 1 minute to capture the DNA on the silica membrane. The flow-through was discarded, and 600 µl of Wash Buffer was added to the column. The column was centrifuged again at 5000 rpm for 1 minute, and the flow-through was discarded. An additional 200 µl of Wash Buffer was added, and the column was centrifuged at 5000 rpm for another minute to ensure thorough washing.

To dry the silica membrane, the column was centrifuged at 14000 rpm for 1 minute. The column was then transferred to a new 1.5 ml microcentrifuge tube, and 100 µl of Elution Buffer was added directly onto the silica membrane. The column was allowed to sit at room temperature for 1 minute to allow the DNA to elute. Finally, the column was centrifuged at 10000 rpm for 1 minute to collect the purified plasmid DNA in the microcentrifuge tube.

The purified plasmids were stored at -5°C in a refrigerator for future use, such as agarose gel electrophoresis, midi prep, and HEK 293 cell transfection. Only plasmids that showed positive results in agarose gel electrophoresis were kept for further analysis and experiments.

3.1.8 Midi Prep Procedure

For the midi prep procedure, first pick a single colony from the agar plate and pre-culture it in 2 ml of LB medium containing ampicillin or kanamycin for several hours. The pre-culture was then transferred to 100 ml of LB medium with the same antibiotic and incubated overnight at 37°C.

The bacterial culture was harvested in a 50 ml centrifuge tube by centrifuging at 7000 rpm for 5 minutes. The supernatant was discarded, and the pellet was resuspended in 8 ml of Resuspension Buffer (RES) using a vortex mixer. Next, 8 ml of Lysis Buffer (LYS EF) was added, and the contents were mixed until the solution turned blue, indicating the start of cell lysis. After waiting for 2-3 minutes, 8 ml of Neutralization Buffer (NEU EF) was added, turning the solution from blue to whitish, indicating successful neutralization.

Figure 6 : Column setting for midi prep

The tube was centrifuged at 10000 rpm for 5 minutes to separate the cell debris. The clear supernatant containing the plasmid DNA was collected and poured into a chromatography column with a filter on a black stand. The column was equilibrated with 15 ml of Equilibration Buffer (EQU EF). After the supernatant passed through the filter, the column was washed with 5 ml of Wash Buffer (WASH EF) to remove any remaining impurities. The filter column was then discarded.

Next, 35 ml of Endotoxin Removal Buffer (ENDO EF) was added to the new column to remove endotoxins. Afterward, 15 ml of Wash Buffer (WASH EF) was added to further purify the DNA. A new 50 ml collection tube was placed beneath the column, and 5 ml of Elution Buffer was added to elute the plasmid DNA. To precipitate the DNA, the eluate was transferred to a new tube, and 5 ml of isopropanol (IPA) was added. The mixture was gently vortexed and centrifuged at 15000 rpm for 30 minutes to form a transparent crystalline pellet.

The supernatant was carefully discarded, and the pellet was washed with 70% ethanol (EtOH) to remove residual impurities. After a gentle vortex mix, the tube was centrifuged again at 15000 rpm for 10 minutes. The ethanol was discarded, and the pellet was air-dried for a few minutes to ensure complete evaporation of the ethanol. Finally, the DNA pellet was dissolved in 100 µl of TE Buffer (TE EF), and the concentration was measured.

3.2 Polycistronic expression; P2A peptide

Polycistronic expression (in eukaryotes) = “one promoter, two or more separate proteins.”

A single mRNA is transcribed from one promoter, yet it encodes several independent open reading frames (ORFs). After translation each ORF gives rise to a distinct, fully functional polypeptide.

Prokaryotes can do it naturally with operons, but eukaryotes need to use 2A peptides(P2A), IRES, or split-inteins to let the ribosome either skip at the 2A motif to release the upstream protein and re-initiate downstream (P2A, T2A, etc.), or– re-initiate at an IRES (Abdi Ghavidel et al., 2022).

In this research, the P2A peptide has one job only—“to turn a single mRNA into two independent, fully functional proteins. I built a single open-reading frame that encodes Spot-cNrxn1βΔECD2–P2A–EGFP-Rab3: upstream lies the engineered, membrane-anchored synapse organizer Spot-cNrxn1βΔECD2; downstream is the presynaptic vesicle marker EGFP-Rab3; and bridging them is the self-cleaving P2A peptide. During translation, ribosome skipping at the P2A motif cleaves the nascent polypeptide into two independent proteins—Spot-cNrxn1βΔECD2 remains in the plasma membrane, while EGFP-Rab3 is released and traffics to synaptic vesicles. This polycistronic design allows both proteins to be expressed from a single transcript after one transfection, preventing the mis-localization and background signal that would arise if EGFP-Rab3 were fused to the membrane protein. As a result, EGFP-Rab3 puncta faithfully report presynaptic differentiation sites and yield an unambiguous Rab3 index. In short, the P2A peptide functions as a molecular scissor that ensures simultaneous yet completely separate expression of the synapse organizer and its fluorescent reporter.

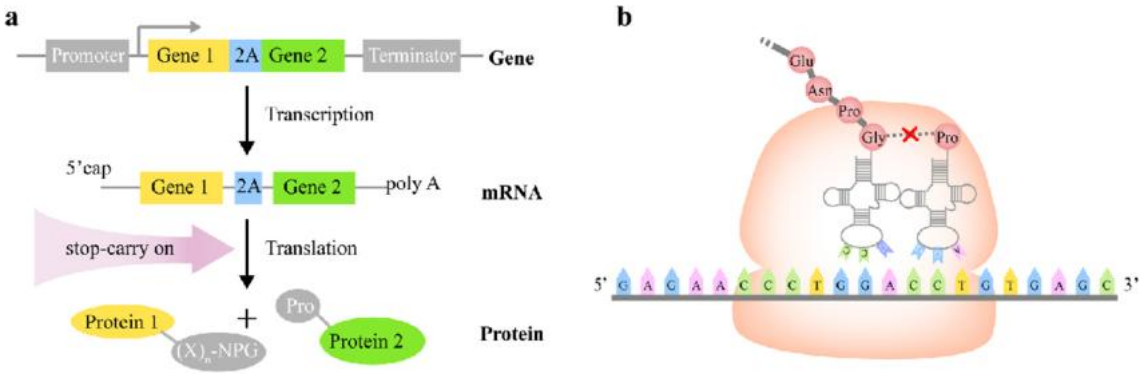

Fig.7 P2A self-cleaving splitting (Synthetic and Systems Biotechnology10(8) September 2024)

3.3 DE3 based protein expression in E-Coli and purification

The DE3 strain is a general term for Escherichia coli that integrates the λ DE3 lysogenic bacteriophage on its chromosome. The λ DE3 bacteriophage carries the T7 RNA polymerase gene and is placed under the control of the lacUV5 promoter; Therefore, when IPTG is added to the culture medium, a large amount of T7 RNA polymerase is synthesized, which drives efficient transcription of any plasmid carrying the T7 promoter. Simply put, "DE3" represents the marker that can activate the T7 expression system under IPTG induction (Shilling et al., 2020).

Protein Preparation from bacterial culture (midi scale, 25ml, uses BugBuster)

(day 0) Transform bacteria expression plasmid (ex pRsetB) to JM109DE3 (or DH5(DE3)),

(day 1) pick a single colony and culture in 25ml (LB+Amp) shake at 27C; for 3 nights; 150 rpm;

(day 4; after 3 nights) harvest cells (spin at 5000rpm; 5min) in a 15ml tube, Wash by re-suspending with 10ml PBS and spin again; Freeze the pellet at -80.

① Suspend bacteria pellet completely with 1ml BugBuster; use vortex

② Shake at room temp for 20-30 min

③ Transfer into 1.5ml; Centrifuge at 14000rpm, 15 min, 4C,

④ Take supernatant to a new 1.5ml tube

⑤ Well re-suspend Talon-resin in the bottle; then 160ul Talon into the tube from #4,

⑥ rotate at 4C for several hours (or overnight)

⑦ 1st wash; Spin at 2000 rpm, 3 min to sink down the resin Discard supernatant only very carefully; put 1.2 ml PBS+ 2.5mM Imidazole, rotate at 4C for 5-10 min

⑧ 2nd wash; Repeat #7

⑨ Spin at 2000 rpm, 3 min to sink down Talon;, Discard supernatant only very carefully; put 1.0ml PBS+ 0.5M Imidazole, rotate at 4C for 5-10 min

⑩ Spin at 2000 rpm, 3 min to sink down Talon; TAKE supernatant only very carefully into a new 1.5ml tube (=1st elution), put 1.0 ml PBS+ 0.5M Imidazole, rotate at 4C for 5-10 min

⑪ Spin at 2000 rpm, 3 min to sink down Talon; TAKE supernatant only very carefully into a new 1.5ml tube (=2nd elution)

⑫ Use a VIVA clear to filter the harvests (i.e. tubes from #10 and #11). Can process 0.5ml at once. Therefore, do repeat.

⑬ Use a VIVA-Spin of proper pore size to concentrate and complete buffer exchange to PBS; final volume 30~40ul.

3.4 Preparation of Fc fusion proteins in HEK293 cells

Fc fusion protein is a type of chimeric molecule formed by genetic or chemical fusion of Fc fragments of IgG antibodies with other functional proteins/peptides. The Fc segment provides dimerization framework, long circulating half-life, affinity purification gripper, and immune effector function, while the fused functional domain confers targeting, antagonizing, capturing, labeling, or therapeutic activity (Czajkowsky et al., 2012). In order to fuse the anti-Spot/V5/Alfa nanobody gene with human IgG1 Fc fragment and generate nanobody Fc fusion protein. Using the high affinity between Fc and Protein A, the supernatant was collected 48-72 hours after transfection and purified in one step by affinity chromatography of Protein A to obtain a working concentration of approximately 5 μ g/mL for cell binding experiments and bead functionalization (Haga et al. 2024; Hamid et al. 2023).

Firstly, the cDNA encoding anti-BC2 nanobody (referred to as anti-SpotNb in the article) was cloned into a fusion expression vector containing human IgG1 Fc fragment, and then the plasmid was transiently transfected into HEK293 cells using Lipofectamine 3000. After transfection, the concentration of fetal bovine serum in the culture medium was reduced to 2%, and the culture continued for 48-72 hours to allow the Fc fusion protein to be secreted into the supernatant. Then collect the culture supernatant and filter it through a 0.22 μ m needle filter to remove cell debris.

Finally, the filtered supernatant was incubated overnight at 4 ° C with Protein-A magnetic beads (PAMS-40-S, 4.7 μ m) to capture the Fc fusion protein through its high affinity for Protein A; After thorough washing, the magnetic beads can be directly used for subsequent bead neuron co culture experiments, or purified proteins can be obtained by

elution.

3.5 Preparation and culture of chick forebrain neurons

In the experiment, Imayasu-san provided me with the greatest help in neuronal preparation. We conducted the following experiments based on Imayasu-san's neuronal preparation process.

1. Chicken embryo incubation

Incubate locally sourced fertilized eggs in a 38 ° C incubator for 8-9 days until embryonic stage E8-E9.

2. Forebrain sampling

Take out the intact forebrain in ice PBS (without Ca^{2+}/Mg^{2+}), place it in 2 mL of ice PBS, and remove the meninges.

3. Mechanical shredding

Cut the forebrain into small pieces of<0.5 mm^3 using a surgical blade.

4. enzymatic digestion

Add a mixture of 0.05% trypsin (Nacalai Tesque) and 10 U DNAse I (Takara Bio) in PBS, digest at 37 ° C for 7 minutes, and gently shake during the process.

5. Mechanical dissociation

Gently blow with a pipette to disperse the tissue into a single-cell suspension.

6. Filtration centrifugation

After filtering through a 100 μ m cell sieve, centrifuge at 1000 rpm for 10 minutes and

discard the supernatant.

7. Suspension and vaccination

Resuspend MEM (Sigma M4655) containing 2% FBS and 1% B27, and inoculate at a density of approximately 1×10^5 cells/cm ^{2} onto Ø 12 mm glass slides pre coated with equal amounts of poly-L-lysine (1 mg/mL) and poly-D-lysine (0.1 mg/mL).

8. Fluid exchange and maintenance

The next day, the culture medium was replaced with MEM containing 2% horse serum and 1% B27. Subsequently, the culture can be continued with or without CO_2 and transfected into DIV4. This chick forebrain neurons exhibit synaptogenic responses compatible with rat cortical neurons, providing a practical cellular model for engineered synapse–microelectrode interface studies.

3.6 Gene delivery via lipofection

Gene delivery in chick forebrain neurons via lipofection protocol

1. Fertilized eggs incubated at 38 °C for 8–9 days (E8–E9).Forebrains dissected in ice-cold Ca^{2+}/Mg^{2+}-free PBS, meninges removed.

2. Tissue minced <0.5 mm³, then digested 7 min at 37 °C with 0.05 % trypsin + 10 U DNAase I.

3. Gentle trituration → 100 µm strainer → 1 000 rpm, 10 min spin.

4. Plate on poly-L/D-lysine-coated Ø12 mm coverslips at ~1×10^5 cells cm^{-2} in MEM + 2 % FBS + 1 % B27.

5. Medium changed next day to MEM + 2 % horse serum + 1 % B27; cultures maintained at 37 °C (5 % CO_2) or 25 °C (CO_2-independent L-15).Transfection performed at DIV 4.

6. Lipofection mix (per 24-well or Ø12 mm coverslip), 0.8–1 µg plasmid (e.g. pCAG-EGFP, pCAG-Spot-mNrxn1βΔECD) in 50 µL Opti-MEM.2 µL Lipofectamine 3000 (Invitrogen) in 50 µL Opti-MEM.

7. Combine 1:1, incubate 15 min RT to form lipoplexes. Replace neuron medium with 400 µL Opti-MEM per well. Add lipoplexes dropwise, mix gently. Incubate 4–6 h (37 °C or 25 °C). Replace with complete growth medium; analyze 24–48 h later.

EGFP fluorescence detectable within 4 h; maximal expression at 24 h. Neurons retain healthy morphology with elongated neurites for ≥10 days post-lipofection.

This protocol reliably yields 20–30 % transfected chick forebrain neurons under both standard incubator and CO_2-independent conditions, enabling rapid gene-function studies and prototyping of neuron-microelectrode interfaces.

3.7 Gene delivery via electroporation

The electroporation experiment was set up by preparing the electroporation cuvettes and setting the voltage conditions. 100 µL of the cell suspension was added to the cuvette, gently tapped to ensure even cell distribution, and placed into the electroporation chamber. Before starting, the resistance of the cuvette was measured, aiming for an ideal resistance of around 550 ohms or lower. If the resistance was too high, more Opti-MEM was added to the cuvette to reduce it. Once everything was ready, the "START" button was pressed to apply the electric pulse for electroporation.

In this experiment, there are four kinds of electroporation voltage diagrams to be applied. I named these four kinds of diagrams A,B,C,D respectively. The following table is the specific values of Diagrams.

Cell's name: chick forebrain primary neuron Primary cultured nerve cells from chicken fetal forebrain												
Sample	Set value											
	Poring Pulse(Pp)						Transfer Pulse(Tp)					
	Voltage V	**pulse width** ms	**pulse interval** ms	**frequency**	**Attenuation rate** %	**polar**	**voltage** V	**pulse width**	**pulse interval** ms	**frequency**	**Attenuation rate** %	**polar**
A	275	0.5	50	2	10	+	20	50	50	5	40	+/-
B	275	1	50	2	10	+	20	50	50	5	40	+/-
C	275	0.5	50	3	40	+	10	2	50	5	10	+/-
D	285	1	50	2	10	+	20	50	50	5	40	+/-

Chart 1: Electroporation Voltage Condition Diagram

3.8 Epi-fluorescence and Laser Scanning Microscopy

Epi-fluorescence observation (wide-field fluorescence imaging) is the simplest and fastest way to visualize fluorescent signals in cells, tissues, or engineered devices like the neuron-microelectrode constructs described in the earlier papers(Combs, 2010).

First, choose filter set to match excitation (Ex) and emission (Em) maxima of your fluorophore (e.g., EGFP: Ex 470/40 nm, Em 525/50 nm)v, then I can verify that the dichroic mirror cut-off is between the two.

Acquisition sequence

① Focus in bright-field to locate the region.

② Switch to fluorescence; adjust field diaphragm to avoid scattered light.

③ Single-channel or multi-channel (EGFP + Alexa 594) capture; save 16-bit TIFF..

Quick quality checks

① Positive control: transfected EGFP plasmid should show cytoplasmic signal in 24 h.

② Negative control: same cells without EGFP (or with scrambled plasmid) should be dark.

③ Background subtraction: draw a region outside the cell in FIJI/ImageJ and subtract mean intensity.

In summary, epi-fluorescence observation is a quick, low-cost method ideal for rapid assessment of transfection efficiency, synapse marker accumulation (e.g., EGFP-Rab3 puncta), or bead-neuron contacts. When deeper optical sections or 3-D reconstruction is required, switch to Laser Scanning Microscopy.

Laser Scanning Microscopy (LSM) – also called laser-scanning confocal microscopy – is the workhorse technique for obtaining high-contrast, optically sectioned fluorescence images in chick forebrain neurons, HEK293 cells, or any 3-D specimen thicker than ~5 μm.

Physical principle

① A diffraction-limited laser spot is raster-scanned across the sample.

② A variable pinhole placed at a conjugate focal plane blocks out-of-focus light, so only

photons originating from the chosen z-plane reach the detector (photomultiplier tube, GaAsP, or hybrid detector).

Crisp optical slices (axial resolution ≈ 500–700 nm) that can be stacked into 3-D volumes. In short, laser scanning confocal microscopy converts your chick forebrain cultures into crisp 3-D datasets, enabling precise mapping of synaptic organizers, bead–neuron contacts, or gene-expression patterns without physical sectioning.

3.9 Shapiro–Wilk test of normality

The Shapiro Wilk test of normality is a statistical test method used to determine whether a sample comes from a normally distributed population. It was proposed by Samuel Sanford Shapiro and Martin Wilk in 1965 and is considered one of the effective methods for testing normality, particularly suitable for small sample situations (SHAPIRO & WILK, 1965).

The Shapiro–Wilk test tests the null hypothesis that a sample x_1, ..., x_n came from a normally distributed population. The test statistic is

$$W = \frac{\left(\sum_{i=1}^{n} a_i x_{(i)}\right)^2}{\sum_{i=1}^{n} (x_i - \bar{x})^2},$$

where

- $x_{(i)}$ with parentheses enclosing the subscript index i is the i-th order statistic, i.e., the i-th-smallest number in the sample.
- $\bar{x} = (x_1 + \cdots + x_n) / n$ is the sample mean.

The coefficients a_i are given by:

$$(a_1, \dots, a_n) = \frac{m^\top V^{-1}}{C}$$

where C is a vector norm:

$$C = V^{-1}m = (m^\top V^{-1} V^{-1} m)^{1/2}$$

and the vector m:

$$m = (m_1, \dots, m_n)^T$$

is made of the expected values of the order statistics of independent and identically

distributed random variables sampled from the standard normal distribution; finally, V is the covariance matrix of those normal order statistics.

The null-hypothesis of this test is that the population is normally distributed. If the p value is less than the chosen alpha level, then the null hypothesis is rejected and there is evidence that the data tested are not normally distributed.

In this experiment, I need to compare the differences in Rab3 index (Ibead/Aixon-1) under 9 experimental conditions (3 constructs x 3 nanobodies). Due to the requirement for data to follow a normal distribution in subsequent parameter tests (such as one-way ANOVA), they first conducted a premise check using Shapiro Wilk.

The experimental sample size is 12-54 contact points per condition, belonging to the small to medium sample range, which is exactly the most suitable range for Shapiro Wilk.

Due to some groups having $p<0.05$, I abandoned parametric testing and switched to Kruskal Wallis testing + Dunn's multiple comparison test.

3.10 Kruskal–Wallis test

The Kruskal–Wallis test is a non-parametric statistical procedure used to determine whether three or more independent samples originate from the same underlying population distribution (i.e., to test for significant differences among groups). It does not require the assumption of normality or homogeneity of variances and serves as the non-parametric alternative to one-way ANOVA (Kruskal & Wallis, 1952).

Rank all data from all groups together; i.e., rank the data from 1 to *N* ignoring group membership. Assign any tied values the average of the ranks they would have received had they not been tied.

The test statistic is given by

$$H = (N-1)\frac{\sum_{i=1}^{g} n_i(\bar{r}_i - \bar{r})^2}{\sum_{i=1}^{g}\sum_{j=1}^{n_i}\left(r_{ij} - \bar{r}\right)^2}$$

Where

- N is the total number of observations across all groups
- g is the number of groups
- n_i is the number of observations in group i
- r_{ij} is the rank (among all observations) of observation j from group i
- $\bar{r}_{i\cdot} = \frac{\sum_{j=1}^{n_i} r_{ij}}{n_i}$ is the average rank of all observations in group i
- $\bar{r} = \frac{1}{2}(N+1)$ is the average of all the r_{ij}.

If the data contains no ties, the denominator of the expression for H is exactly $(N-1)N(N+1)\,/\,12$ and $\bar{r} = \frac{N+1}{2}$. Thus

$$H = \frac{12}{N(N+1)}\sum_{i=1}^{g} n_i \left(\bar{r}_{i\cdot} - \frac{N+1}{2}\right)^2 = \frac{12}{N(N+1)}\sum_{i=1}^{g} n_i \bar{r}_{i\cdot}^2 - 3(N+1)$$

The last formula contains only the squares of the average ranks.

Finally, the decision to reject or accept the null hypothesis is made by comparing *H* to a critical value *Hc* (obtained from a table or software) for a given significance or alpha level.

After Shapiro–Wilk tests revealed non-normality ($p < 0.05$) for some conditions, I applied the Kruskal–Wallis test to compare nine experimental groups, confirming the orthogonality of the three engineered synapse organizers.

3.11 Dunn's multiple comparison test

If the statistic is not significant, there is no evidence of stochastic dominance among the samples. However, if the test is significant then at least one sample stochastically dominates another sample. Then, a researcher might use sample contrasts between individual sample pairs, or *post hoc* tests using Dunn's test, which properly employs the same rankings as the Kruskal–Wallis test, and properly employs the pooled variance implied by the null hypothesis of the Kruskal–Wallis test in order to determine which of the sample pairs are significantly different. When performing multiple sample contrasts or tests, the Type I error rate tends to become inflated, raising concerns about multiple comparisons.

The Dunn's multiple comparison test is a non-parametric post hoc testing method used to compare pairwise which groups have significant differences after discovering overall differences in the Kruskal Wallis test (Dinno, 2015).

The formula for the Dunn test statistic *Z* when there are no ties (i.e., no identical ranks in the data) is given by:

$$Z = \frac{R_i - R_j}{\sqrt{\frac{N(N+1)}{12}\left(\frac{1}{n_i} + \frac{1}{n_j}\right)}}$$

where:

- *Ri* and *Rj* are the mean ranks of the *i*-th and *j*-th groups, respectively.
- *N* is the total sample size across all groups.
- *ni* and *nj* are the sample sizes of the *i*-th and *j*-th groups, respectively.

When there are ties in the data, Dunn (1964) proposed an adjustment to the standard deviation.

After discovering overall differences in Kruskal Wallis test, I used Dunn test to accurately locate three on target combinations (Spot × anti SpotNb, V5 × anti-V5Nb, Alfa × anti AlfaNb) that were significantly higher than the other off target combinations, verifying the orthogonal selectivity of engineered synaptic organizers.

In the data analysis of this experiment, Professor Tsutsui provided me with tremendous technical support and assistance, including efficient data processing tools and specific data analysis processes. It is precisely because of his help that my experimental results are more specific and realistic.

Chapter 4

Result and Conclusions

4.1 Results

I began this work by using the engineered synapse organizer in our previous report, Spot-cNrxn1βΔECD::P2A-EGFP-Rab314). It is based on a truncated version of chick Neurexin1β (cNrxn1βΔECD), lacking the extracellular domain to prevent binding with natural receptors including neuroligin-1, and instead, carries at the N-terminus a peptide ligand named Spot-tag. It also allows polycistronic expression of EGFP-Rab3 as a fluorescence presynapse marker. To extend the repertoire with multiple epitope tags and constitute a candidate set of orthogonal synaptic organizers, the gene constructs with V5 or Alfa tags instead of Spot tags were generated and were named as V5-cNrxn1βΔECD::P2A-EGFP-Rab3 or Alfa-cNrxn1βΔECD::P2A-EGFP-Rab3, respectively (Fig. 8). Here, the amino acid sequences for Spot, V5 and Alfa-tag are PDRVRAVSHWSS, GKPIPNPLLGLDST, and SRLEEELRRRLTE in the single letter code, respectively (Braun et al. 2016; Götzke et al. 2019; Virant et al. 2018b; Zeghal et al. 2023). Also, nanobodies for these tags are available. Spot-tag is an enhanced ligand for the anti-BC2 nanobody. Therefore, to avoid confusion, anti-BC2 nanobody is referred to as anti-SpotNb in this study. The three constructs, as candidates for orthogonal engineered synapse organizers, were transfected into HEK293T cells to confirm their expression according to the standard protocol described elsewhere (Haga et al. 2024; Hamid et al. 2023).

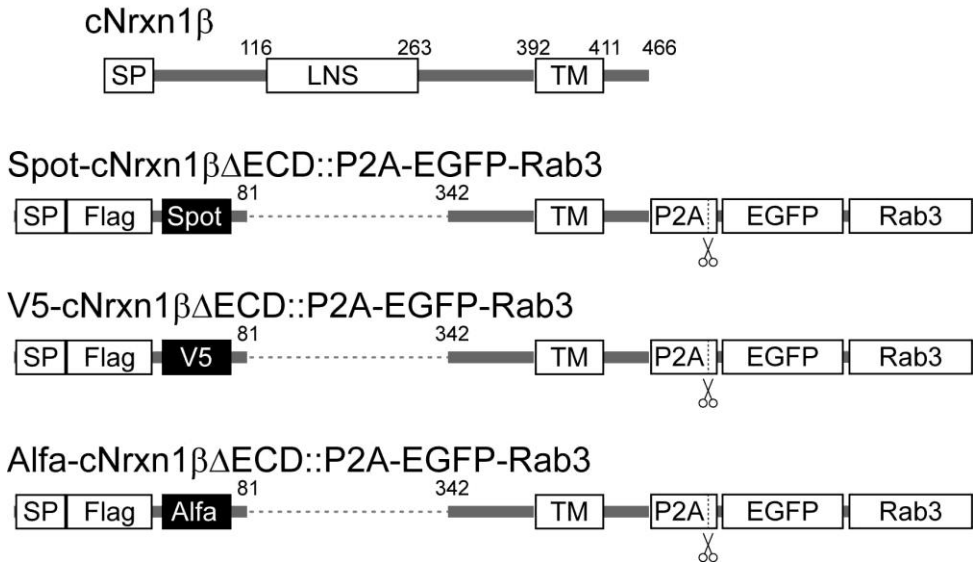

Fig. 8 Design of the orthogonal set of engineered synapse organizers based on chick Nrxn1β and the three peptide tags.

There were no noticeable differences in the fluorescence intensity or distribution of EGFP-Rab3 among these constructs (Fig. 9a). To perform the binding test, nanobody-Fc fusion proteins targeting the tags (i.e. anti-SpotNb_Fc, anti-V5Nb_Fc, and anti-AlfaNb_Fc) were prepared as previously described. HEK293T cells expressing any of the three constructs were then incubated for 3 hours in a medium containing one of the three kinds of nanobody-Fc at the concentration of ~ 5 μg/ml. Cells were washed with phosphate-buffered saline (PBS), fixed with 4% paraformaldehyde, subjected to immunostaining with an anti-human immunoglobulin G antibody (1:3000 dilution) and a secondary antibody conjugated with Alexa Fluor 594 (1:1000 dilution), and imaged using a laser scanning microscope (FV1000D, Evident, Tokyo, Japan). The results qualitatively showed that Spot, V5, and Alfa peptide ligands were presented on the cell surface as designed and were selectively detected by the nanobodies for these tags in a one-to-one

manner (Fig. 9b) (Haga et al., 2024b).

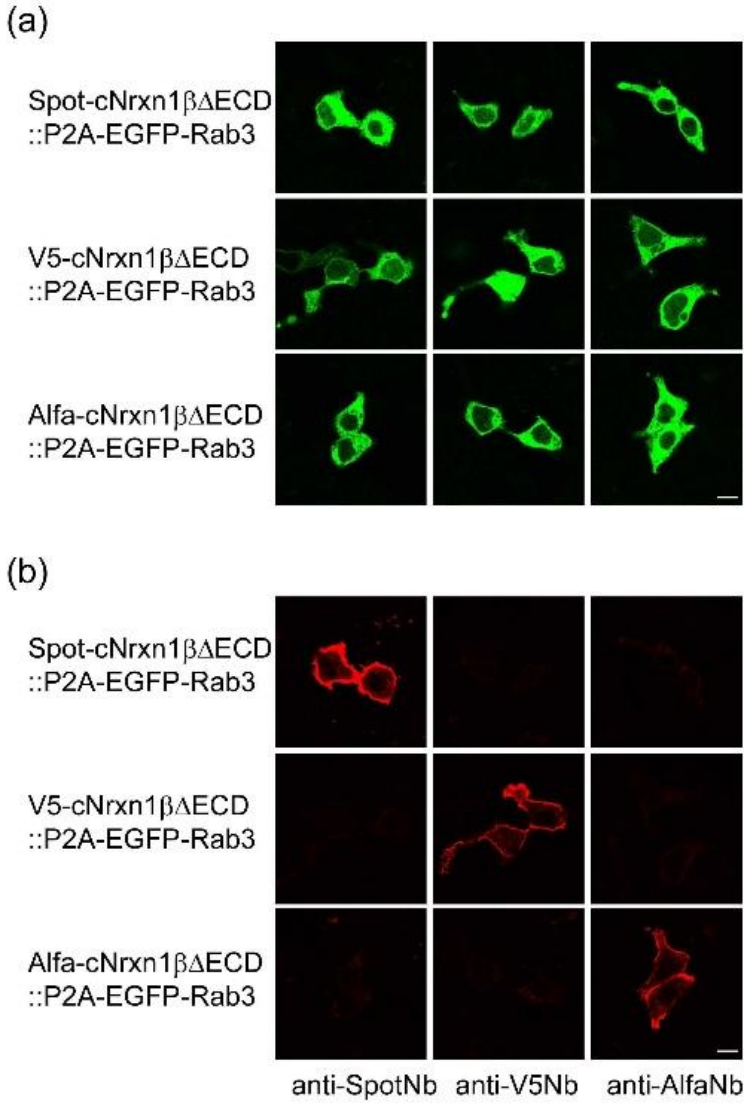

Fig.9 (a) Representative fluorescence images of HEK293T cells expressing the constructs. (b) Binding test of surface epitopes in the same cells shown in panel b with anti-SpotNb-Fc, anti-V5Nb-Fc, or anti-AlfaNb-Fc. Bar = 10 μm; applies to all images.

Although the quantitative binding properties of the three peptide tags and their nanobodies have been reported, their cross-binding properties have not been fully

evaluated.

Therefore, I checked the cross-binding properties of these nanobodies and especially at high concentration of the tags as follows. Excess amount of anti-SpotNb_Fc, anti-V5Nb_Fc, and anti-AlfaNb_Fc (~10 μg) were incubated with ~ 0.1 mg protein-A conjugated magnetic microbeads (PAMS-40-S, Spherotech, Illinois, USA) at 4°C for overnight using a low protein binding microtube. After washing three times with PBS, the nanobody-Fc@protein-A microbead complex was divided into glass-bottom microwells (EZVIEW plate, Fuji Film, Tokyo) and incubated for 3 hours with 0.2 ml PBS containing a defined concentration ranging from 31.25 nM to 8 μM of Venus fluorescent protein fused to the Spot, V5, or Alfa-tag at its C-terminus. Following three washes with 0.2 mL of PBS, the microbeads were analyzed via fluorescence microscopy within 30 minutes to 1 hour. Signals were detected when nanobody-bound microbeads were incubated with Venus carrying the corresponding tag, demonstrating specific binding. Signals reflecting non-specific binding were undetectable, even at the highest concentration (8 μM) of Venus with the off-target tags (Fig. 10d).

In the binding test of anti-SpotNb and anti-V5Nb with their respective ligands, the ligand concentrations giving half-maximal fluorescence were approximately 30 nM (Fig. 10a)and 150 nM(Fig. 10b), respectively, which are several-fold higher than the equilibrium dissociation constants (Kd values) reported. It should be noted that the present assay was performed under non-equilibrium conditions because tagged Venus retained after PBS washing was measured. Additionally, binding characteristics generally depend on the interaction environment, including the host protein for the tag. The half-maximal concentration for anti-AlfaNb was outside the range of ligand concentrations examined, which is consistent with the high-affinity (Kd ~ 26 pM) characteristics in the

interaction between Alfa-tag and its nanobody (Fig. 10c).

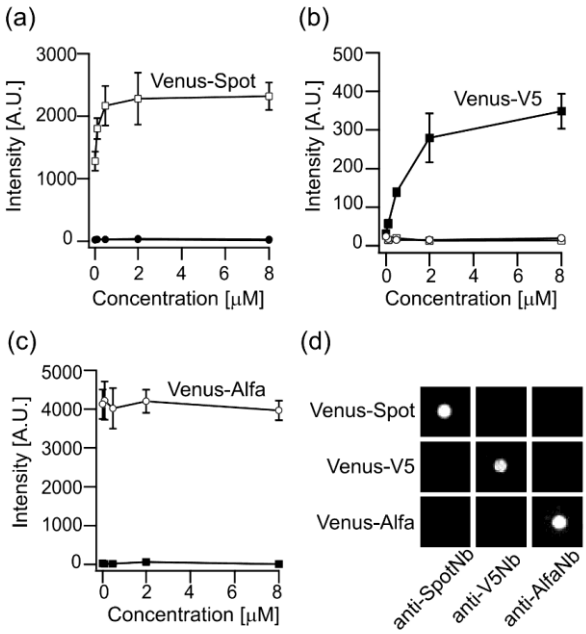

Fig. 10. Fluorescence retained on microbeads immobilized with anti-SpotNb (a), anti-V5Nb (b), and anti-AlfaNb (c) after incubation with Venus-Spot (open square), Venus-V5 (filled square), and Venus-Alfa (open circle) at concentrations ranging from 0.031 to 8 μM. Data are shown as mean ± S.D. for 10 microbeads. (d) Representative images of microbeads with a total of nine combinations at a ligand concentration of 8 μM, shown with the identical intensity scale.

I investigated the synapse-inducing activities of the three constructs (i.e., X-cNrxn1βΔECD::P2A-EGFP-Rab3, where X = Spot, V5, or Alfa tag) in the neuronal circuit to determine whether they function as orthogonal synapse organizers, acting specifically upon interaction with the counterpart nanobody, and also to study whether the activity depends on the type of ligand-nanobody pair. To this end, primary chick forebrain neurons were prepared from 8- or 9-day-old embryos and plated onto φ12 mm coverslips at a density of ~105 cells/cm² (Heidemann et al., 2003). The nanobody-

Fc@protein A microbead composite was used to mimic a microelectrode functionalized with the nanobody. Neurons were transfected with one of the three constructs at 5–6 days of in vitro culture using Lipofectamine 3000 reagent (Thermo Fisher Scientific, MA, USA) according to the manufacturer's protocol. The next day, one of the three nanobody-microbead composites (i.e., anti-SpotNb, anti-V5Nb, or anti-AlfaNb) was added at the density of 105 beads per the coverslip, and co-cultured overnight. After fixation under a total of nine conditions, the samples were mounted on glass slides and subjected to laser scanning microscopy[3] [4]. Neuronal axons expressing the constructs were identified as thin, long processes exhibiting green fluorescence from EGFP-Rab3. In experiments where neurons were co-cultured with microbeads carrying the counterpart nanobody (e.g., construct: Spot-cNrxn1βΔECD; microbeads: anti-SpotNb), EGFP-Rab3 accumulation was frequently detected at axon-microbead contact sites, indicating synaptogenic activity mediated by the peptide-nanobody interaction. In axons contacting off-target nanobodies (e.g., axon: Spot-cNrxn1βΔECD; microbeads: anti-V5Nb), EGFP-Rab3 accumulation was generally substantially less frequent (Fig. 11).

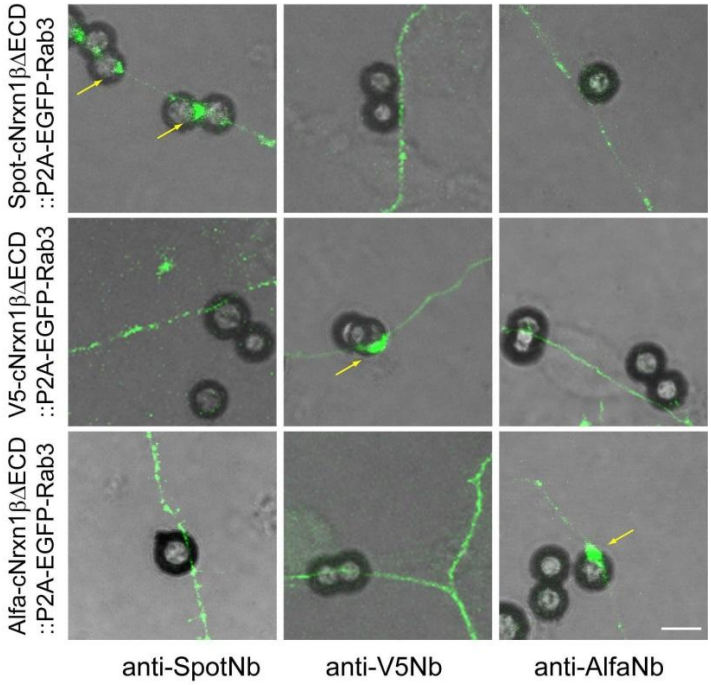

Fig. 11 Representative images of the axon-microbead contact assay for nine combinations of the three constructs and three nanobodies. Bar = 5 μm, applies to all images.

For statistical evaluation, the degree of EGFP-Rab3 accumulation was quantified using a Rab3 index, defined as Ibead/Iaxon-1, where Ibead and Iaxon represent the integrated fluorescence within a 50 μm² circular region around the beads and a representative axon not in contact with the beads, respectively (Fig.12).

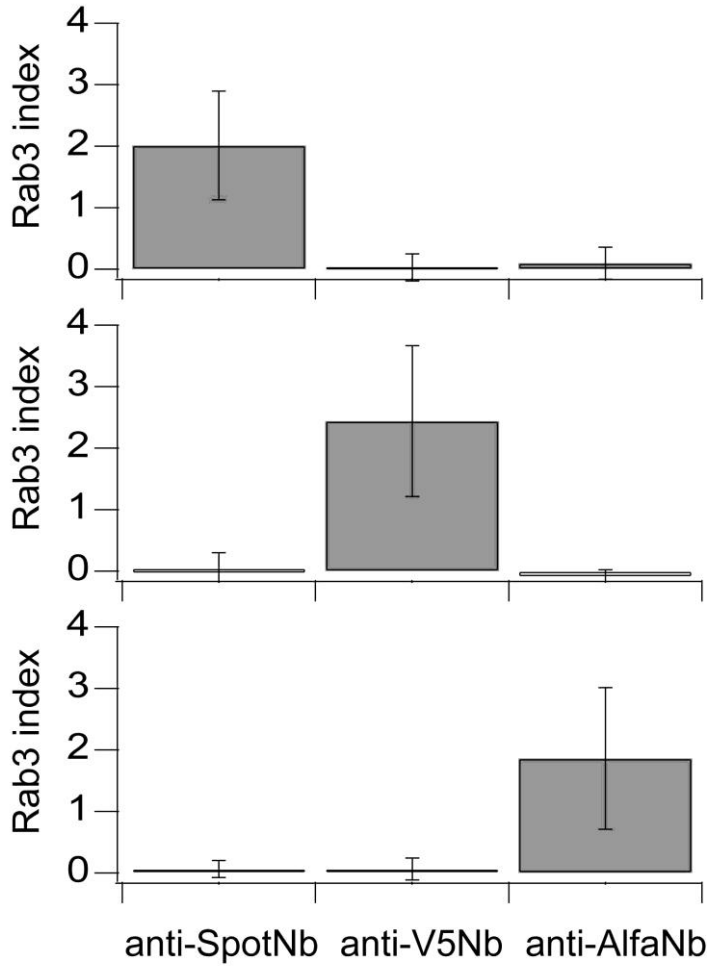

Fig.12 Analysis of the Rab3 index for the corresponding nine different conditions (mean ± S.D.). The number of contacts examined was 22, 14, 13, 12, 27, 13, 16, 13, and 53, from top left to bottom right conditions.

Statistical analysis was performed on randomly selected axon-microbead contacts (n = 12 ~ 54) in 2D images generated by projecting of XYZ-scanned image stacks. Calculations were conducted using R version 4.4.0. Since data in some categories did not pass the Shapiro-Wilk test of normality (p value < 0.05), the Kruskal–Wallis test was performed, followed by Dunn's multiple comparison test. The bindexes for the three target contacts (e.g., axon: Spot-cNrxn1βΔECD; microbeads: anti-SpotNb) were significantly higher than those for the off-target contacts. I did not detect a significant difference in the indexes

among the three target contacts or among the six off-target contracts. Based on these results, I concluded that the three constructs: X-cNrxn1βΔECD::P2A-EGFP-Rab3, where X = Spot, V5, or Alfa tag, function as an orthogonal set of engineered synapse organizers and could be useful for establishing a multiplexed, molecularly inducible neuron-microelectrode interface. It should be noted that the accumulation of EGFP-Rab3 was not always undetectable in the off-target contacts, but minor accumulation seemed to occur in some cases, although these cases did not much affect the result of the statistical analysis. At this stage, there would be two possible explanations. One is that the apparent off-target signals reflect intrinsic synapses at the bead locations (Shipman & Nicoll, 2012), and the other is that there could be some direct basal interaction between axon and micro 8 or 9 d old embryos beads which might stimulate differentiation of presynapse-like structures (Fig.13).

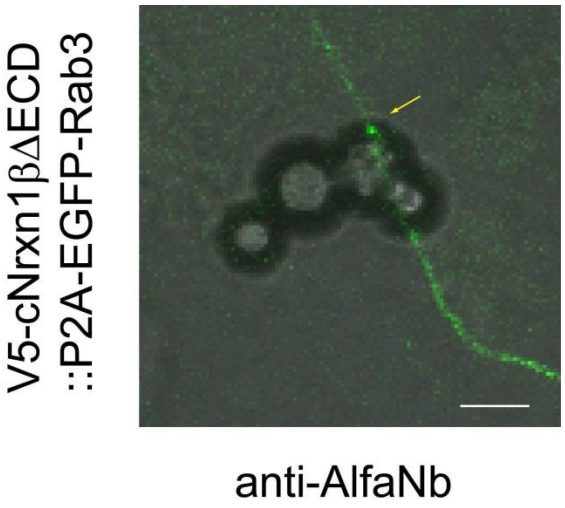

Fig.13 EGFP-Rab3 appears to accumulate slightly in off target contact

While the reported Kd values of the three peptide tags and their nanobodies vary by nearly three orders of magnitude (i.e. 26 pM ~ 29 nM), I did not detect a difference in

the degree of EGFP-Rab3 accumulations at the contacts between axons and microbeads. Nevertheless, considering the above-mentioned mechanism, it is possible that dynamic factors, such as the K_{on} and K_{off} rates of the ligand-nanobody interaction, are correlated with the kinetics and efficiency of the induction of synapse-like structure. Therefore, more precise analysis of synaptogenic activities from such perspective could provide a better microscopic understanding of the process for artificial synaptic organizers and microelectrodes.

4.2 Conclusions

In this study, I demonstrated that the three peptide tags (Spot, V5, and Alfa), each consisting of 12–14 amino acids, can serve as ligands for engineered synapse organizers, which can be selectively activated through interactions with their specific nanobodies. Our analysis showed that the affinity between the ligand and its nanobody required for such a molecular tool is not highly stringent. Since small peptide tags generally have minimal impact on the structure and function of host proteins compared to larger protein epitopes, they provide ideal epitopes for the design of orthogonal molecular tools. Although the number of currently available peptide tags and their corresponding nanobody pairs remains limited, future developments would expand their variety, enabling the development of a larger set of orthogonal engineered synapse organizers. While establishing a multiplexed neuron-microelectrode interface is essential, developing a reliable technique to measure circuit activity through molecularly induced neuron-microelectrode junctions also remains a key challenge. As discussed elsewhere (Hamid et al., 2023; S. Kim et al., 2023), detection of local potentials or activity-dependent transmitter release could form the basis of this methodology. Thus, future research is expected to address these challenges.

Chapter 5

General Discussion and Perspectives

5.1 General Discussion

The core achievement of this paper is to demonstrate that by grafting three small peptide tags (Spot, V5, Alfa) consisting only of 12-14 amino acids onto the truncated neuroexin-1 β skeleton, a set of orthogonal molecular "lock key" switches can be obtained, which can instruct gene defined axons to form functional presynaptic terminals only on the substrate coated with the corresponding nanoantibody. Unlike previous studies that only used a single ligand, this study systematically drew a statistical map of cross reactivity under neuron related conditions for the first time, and established a reproducible standard process from DNA design to chicken neuron validation, elevating the concept of "molecularly induced neuron microelectrode interface" from narrow validation experiments to a potential universal multiplex neural interface platform.

5.2 Perspectives

5.2.1 Expand more number of orthogonal molecular tools

Using artificial intelligence (AI) for de novo design of nanobodies, tools such as RFdiffusion and AlphaFold can be used to design nanobodies with high affinity and specificity based on the structure and characteristics of the target antigen. AI can also quickly identify nanobodies that bind to target antigens and evaluate their binding affinity through high-throughput screening and molecular docking techniques (such as HDOCK), thereby rapidly screening for high affinity candidate molecules.

Through AI assisted high-throughput screening, large-scale nanobody libraries can be constructed, which can contain thousands of different nanobodies. By selectively

mutating and optimizing, the diversity and functionality of the library can be improved. Using AI for functional evaluation can quickly identify nanobodies with specific functions, such as high affinity, high stability, and low immunogenicity.

Finally, AI can integrate data from different experiments and databases to provide comprehensive decision support, helping researchers quickly identify and optimize nanobodies. AI driven automation processes can reduce human errors and improve the repeatability and reliability of experiments. Through these methods, intelligent high-throughput screening technology not only improves the design and production efficiency of nanobodies, but also expands the development of orthogonal molecular tools, providing more powerful tools for neuroscience research and biomedical applications.

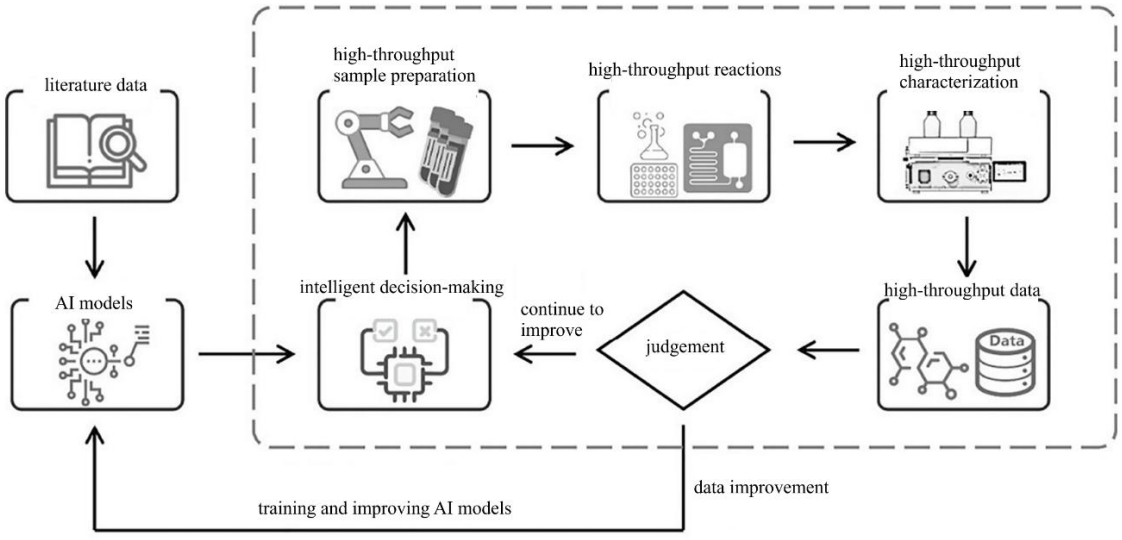

Intelligent high-throughput screening technology for the artificial intelligence.(Chen Jie.et al., 2022, SCIENTIA SINICA CHIMICA)

5.2.2 Cell Biological Insights into Neuron–Microelectrode Junctions

Synapses between neurons are known to undergo a transition from initial synapse formation to mature synapses, which are then maintained by various mechanisms and, depending on the situation, can also be eliminated. In contrast, synapse-like junctions induced by engineered synapse organizers have so far been evaluated only by the accumulation of forcibly expressed EGFP-Rab3, leaving it largely unclear to which stage of synapse development these structures correspond. It also remains unresolved whether the induced presynaptic compartments are excitatory or inhibitory, and whether this depends on the type of artificial synapse organizer employed. Clarifying these issues will be important for developing measurement methods that utilize such synapse-like structures.

With respect to synapse maturation, it is generally considered difficult to assess solely with synaptic markers; instead, whether synaptic vesicle recycling occurs serves as a critical indicator. One of the most suitable experiments to examine this is fluorescence imaging using the dye FM1-43. Regarding neurotransmitter identity, valuable insights could be obtained by examining markers such as vesicular glutamate transporters vGLUT1/2, VGAT (vesicular GABA transporter, SLC32A1), GAD65/67 (isoforms of glutamate decarboxylase), and GlyT2 (glycine transporter 2, SLC6A5).

5.2.3 Development of molecular tools for neuronal circuit editing

We can also explore the development of a molecular tool for precise editing of neural circuits. Based on the previously discovered phenomenon, expressing a modified protein in axons can induce differentiation of presynaptic structures when in contact with microbeads fixed with nanoantibodies. We can design two constructs, one for the presynaptic membrane and one for the postsynaptic membrane, and evaluate synaptic induction activity by expressing these constructs in chicken neuron culture and observing the co localization of fluorescent markers. Although co-localization of presynaptic and postsynaptic markers has been observed at some touchpoints, the possibility that these accumulations are naturally formed synapses cannot be completely ruled out.

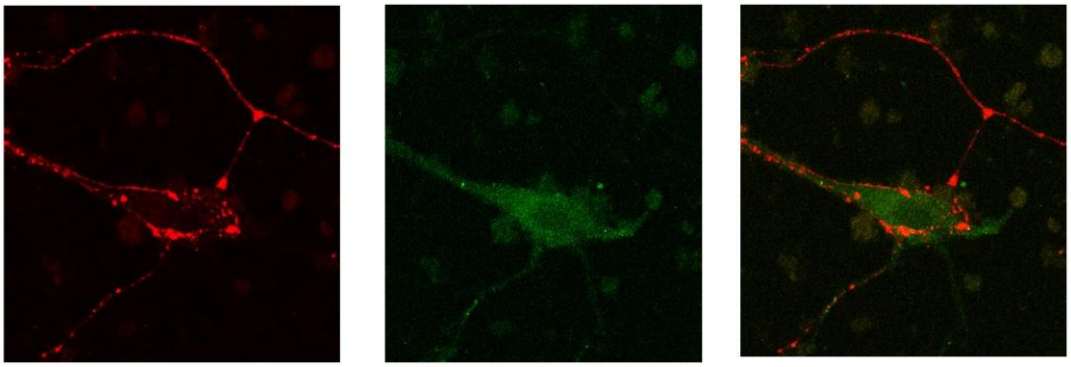

Expression diagram of mCherry and venus fluorescent proteins (Nan Xinyu, 2023)

The research also faces the problem of low gene transfer efficiency, which makes it difficult to observe sufficient contact points and to derive statistically significant differences from control experiments. In the future, it will be necessary to design experimental systems that can quantitatively and statistically evaluate synaptic induction activity, which will require the adoption of more efficient gene transfer methods and more effective neuronal culture protocols.

5.2.4 Real-Time Analysis of the Synaptogenic Process

Understanding the precise sequence of events leading to synapse induction after contact with the beads is crucial for accurately assessing the features, advantages, and limitations of measurement techniques that utilize this junctional structure. Although previous work has investigated the time course of synapse formation (Haga et al. 2024), these studies relied on PFA fixation at predetermined time points after bead addition, leaving the exact timing of bead–neuron contact unresolved. To achieve this objective, optical tweezers are considered the most suitable experimental system. In this technique, focusing laser light through a high-numerical-aperture objective generates forces on micrometer-sized particles due to momentum transfer from photon scattering, allowing them to be trapped. By exploiting this principle, it is expected that contact between beads and axons can be controlled with high precision. In this study, no significant differences in synapse induction were observed among ligand–receptor pairs with different Kd values. However, by precisely controlling bead–axon contact using optical tweezers, it should be possible to compare the rate of synapse formation and the timing of marker accumulation, thereby providing insights into the quantitative aspects of the induction mechanism.

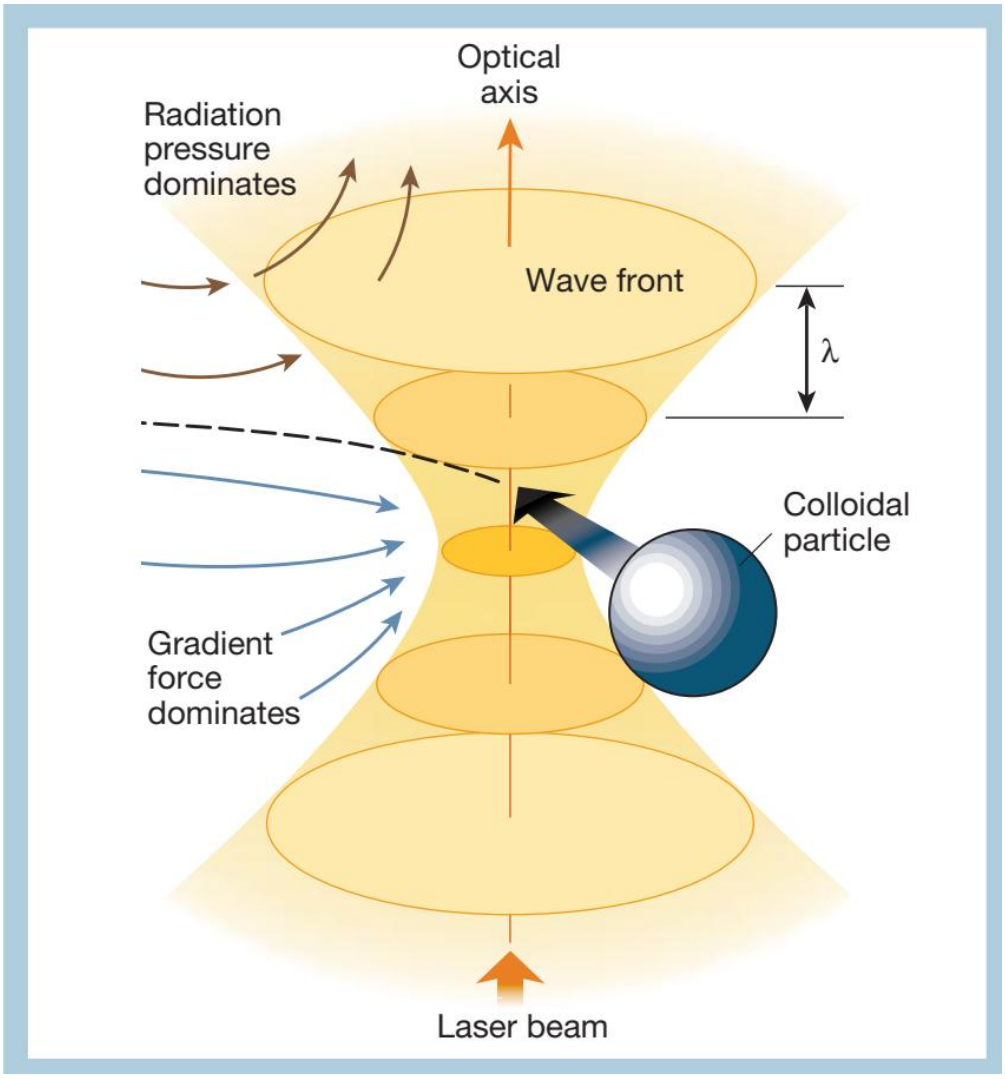

Diagram of Optical Tweezers (Grier, 2003)

5.2.5 Exploring the advanced Applications of Synapse Organizers

The development and application of engineered synapse organizers in brain-computer interfaces (BCIs) hold immense potential for advancing the field of neurotechnology.

Here are several future perspectives on how these organizers can be integrated into BCI systems, particularly in the context of advanced technologies like Neuralink:

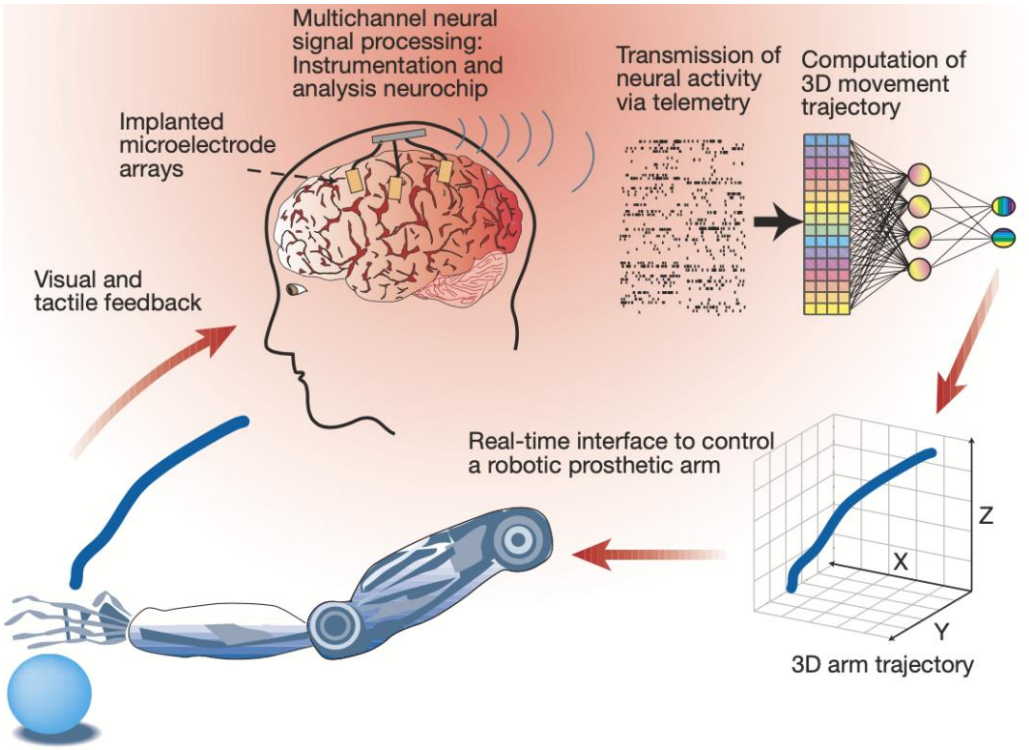

Principle of brain computer interface closed-loop system, taking the movement of brain controlled robotic arm as an example (Nicolelis, 2001)

One of the primary challenges in BCI technology is the acquisition of high-quality neural signals. Engineered synapse organizers can be utilized to enhance the interaction between neurons and electrodes, leading to more stable and robust signal acquisition. By inducing the formation of functional synapses on the surface of microelectrodes, these organizers can significantly improve the signal-to-noise ratio, making it easier to decode neural activity with higher precision.

In BCI systems, the interface between electrodes and neurons is crucial for effective signal transmission. Engineered synapse organizers can be engineered to promote the

growth of synaptic connections specifically at the electrode sites. This targeted induction can lead to more efficient and reliable neural interfacing, potentially reducing the number of electrodes needed and minimizing tissue damage during implantation.

BCI technologies are increasingly being explored for therapeutic applications, particularly in the restoration of sensory and motor functions. Engineered synapse organizers can play a pivotal role in promoting neural repair by facilitating the formation of functional synapses in damaged neural circuits. This application could be particularly beneficial in treating conditions like spinal cord injuries or neurodegenerative diseases, where the restoration of neural connectivity is critical.

As BCI technology continues to evolve, the incorporation of engineered synapse organizers can contribute to the development of next-generation devices. These organizers can be used to create more biocompatible and efficient interfaces, reducing the risk of immune responses and improving long-term stability. This advancement is particularly relevant for invasive BCI systems like Neuralink, where long-term functionality and biocompatibility are paramount.

Conclusive Remarks

In this study, I designed and validated orthogonal engineered synapse organizers, demonstrating that the three peptide tags—Spot, V5, and Alfa—each interact exclusively with their cognate nanobodies. Surface display analysis in HEK293T cells and validation in primary cultured neurons confirmed the absence of cross-reactivity among distinct ligand–nanobody pairs. Despite differences in reported dissociation constants spanning three orders of magnitude, all three organizers exhibited comparable synaptogenic efficiency, regarding EGFP-Rab3 accumulations. These findings establish Spot, V5, and Alfa peptide tags as an orthogonal triplet suitable for multiplexed neural interfaces. This work provides a molecular foundation for cell-type-specific interrogation of neuronal circuits based on genetic identity, and it is expected to facilitate the development of precise, multi-channel electrophysiological recording technologies. Beyond advancing fundamental insights into neural circuit organization, this innovation may also contribute in future to translational applications in neural disease models .

References

[1] R. H. Roth and J. B. Ding, "From Neurons to Cognition: Technologies for Precise Recording of Neural Activity Underlying Behavior," *BME Front*, vol. 2020, Jan. 2020, doi: 10.34133/2020/7190517.

[2] G. H. Kim *et al.*, "Recent Progress on Microelectrodes in Neural Interfaces," *Materials*, vol. 11, no. 10, p. 1995, Oct. 2018, doi: 10.3390/ma11101995.

[3] G. Buzsáki, "Large-scale recording of neuronal ensembles," *Nat Neurosci*, vol. 7, no. 5, pp. 446–451, May 2004, doi: 10.1038/nn1233.

[4] J. Zhang, J. Xia, and H. Xiong, "Techniques for Extracellular Recordings," 2014, pp. 325–345. doi: 10.1007/978-1-4614-8794-4_23.

[5] K. D. Harris, R. Q. Quiroga, J. Freeman, and S. L. Smith, "Improving data quality in neuronal population recordings," *Nat Neurosci*, vol. 19, no. 9, pp. 1165–1174, Sep. 2016, doi: 10.1038/nn.4365.

[6] G. Hong and C. M. Lieber, "Novel electrode technologies for neural recordings," *Nat Rev Neurosci*, vol. 20, no. 6, pp. 330–345, Jun. 2019, doi: 10.1038/s41583-019-0140-6.

[7] K. D. Harris and T. D. Mrsic-Flogel, “Cortical connectivity and sensory coding,” *Nature*, vol. 503, no. 7474, pp. 51–58, Nov. 2013, doi: 10.1038/nature12654.

[8] T. C. Südhof, “Towards an Understanding of Synapse Formation,” *Neuron*, vol. 100, no. 2, pp. 276–293, Oct. 2018, doi: 10.1016/j.neuron.2018.09.040.

[9] P. Scheiffele, J. Fan, J. Choih, R. Fetter, and T. Serafini, “Neuroligin Expressed in Nonneuronal Cells Triggers Presynaptic Development in Contacting Axons,” *Cell*, vol. 101, no. 6, pp. 657–669, Jun. 2000, doi: 10.1016/S0092-8674(00)80877-6.

[10] Sm. A. Hamid, M. Imayasu, T. Yoshida, and H. Tsutsui, “Epitope-tag-mediated synaptogenic activity in an engineered neurexin-1β lacking the binding interface with neuroligin-1,” *Biochem Biophys Res Commun*, vol. 658, pp. 141–147, May 2023, doi: 10.1016/j.bbrc.2023.03.063.

[11] Y. Xing, C. Zan, and L. Liu, “Recent advances in understanding neuronal diversity and neural circuit complexity across different brain regions using single-cell sequencing,” *Front Neural Circuits*, vol. 17, Mar. 2023, doi: 10.3389/fncir.2023.1007755.

[12] M. Zhang *et al.*, “Molecularly defined and spatially resolved cell atlas of the whole

mouse brain," *Nature*, vol. 624, no. 7991, pp. 343–354, Dec. 2023, doi: 10.1038/s41586-023-06808-9.

[13] M. N. Economo, T. Komiyama, Y. Kubota, and J. Schiller, "Learning and Control in Motor Cortex across Cell Types and Scales," *The Journal of Neuroscience*, vol. 44, no. 40, p. e1233242024, Oct. 2024, doi: 10.1523/JNEUROSCI.1233-24.2024.

[14] D. Virant *et al.*, "A peptide tag-specific nanobody enables high-quality labeling for dSTORM imaging," *Nat Commun*, vol. 9, no. 1, p. 930, Mar. 2018, doi: 10.1038/s41467-018-03191-2.

[15] M. B. Braun *et al.*, "Peptides in headlock – a novel high-affinity and versatile peptide-binding nanobody for proteomics and microscopy," *Sci Rep*, vol. 6, no. 1, p. 19211, Jan. 2016, doi: 10.1038/srep19211.

[16] M. Zeghal *et al.*, "Development of a V5-tag–directed nanobody and its implementation as an intracellular biosensor of GPCR signaling," *Journal of Biological Chemistry*, vol. 299, no. 9, p. 105107, Sep. 2023, doi: 10.1016/j.jbc.2023.105107.

[17] H. Götzke *et al.*, "The ALFA-tag is a highly versatile tool for nanobody-based bioscience applications," *Nat Commun*, vol. 10, no. 1, p. 4403, Sep. 2019, doi:

10.1038/s41467-019-12301-7.

[18] J. W. Bigbee, “Cells of the Central Nervous System: An Overview of Their Structure and Function,” 2023, pp. 41–64. doi: 10.1007/978-3-031-12390-0_2.

[19] P. E. Ludwig, V. Reddy, and M. A. Varacallo, *Neuroanatomy, Neurons*. 2025.

[20] J. E. Gentile, M. G. Carrizales, and A. J. Koleske, “Control of Synapse Structure and Function by Actin and Its Regulators,” *Cells*, vol. 11, no. 4, p. 603, Feb. 2022, doi: 10.3390/cells11040603.

[21] S. A. Connor and T. J. Siddiqui, “Synapse organizers as molecular codes for synaptic plasticity,” *Trends Neurosci*, vol. 46, no. 11, pp. 971–985, Nov. 2023, doi: 10.1016/j.tins.2023.08.001.

[22] “Molecular Structure and Engineering of Synaptic Organizer Proteins in Health and Disease,” Mar. 01, 2020. doi: 10.3030/850820.

[23] K. Xue *et al.*, “Using structural analysis to clarify the impact of single nucleotide variants in neurexin/neuroligin revealed in clinical genomic sequencing,” *J Biomol Struct Dyn*, vol. 40, no. 17, pp. 8085–8099, Nov. 2022, doi: 10.1080/07391102.2021.1907225.

[24] E. G. Stokes, H. Kim, J. Ko, and J. Aoto, "A Systematic Structure-Function Characterization of a Human Mutation in Neurexin-3 α Reveals an Extracellular Modulatory Sequence That Stabilizes Neuroligin-1 Binding to Enhance the Postsynaptic Properties of Excitatory Synapses," *The Journal of Neuroscience*, vol. 44, no. 41, p. e1847232024, Oct. 2024, doi: 10.1523/JNEUROSCI.1847-23.2024.

[25] T. C. Südhof, "Neuroligins and neurexins link synaptic function to cognitive disease," *Nature*, vol. 455, no. 7215, pp. 903–911, Oct. 2008, doi: 10.1038/nature07456.

[26] K. Ichtchenko *et al.*, "Neuroligin 1: A splice site-specific ligand for β -neurexins," *Cell*, vol. 81, no. 3, pp. 435–443, May 1995, doi: 10.1016/0092-8674(95)90396-8.

[27] J. Ko, M. V. Fuccillo, R. C. Malenka, and T. C. Südhof, "LRRTM2 Functions as a Neurexin Ligand in Promoting Excitatory Synapse Formation," *Neuron*, vol. 64, no. 6, pp. 791–798, Dec. 2009, doi: 10.1016/j.neuron.2009.12.012.

[28] J. M. Yau, G. C. DeAngelis, and D. E. Angelaki, "Dissecting neural circuits for multisensory integration and crossmodal processing.," *Philos Trans R Soc Lond B*

Biol Sci, vol. 370, no. 1677, p. 20140203, Sep. 2015, doi: 10.1098/rstb.2014.0203.

[29] H. Tsutsui, S. Karasawa, Y. Okamura, and A. Miyawaki, "Improving membrane voltage measurements using FRET with new fluorescent proteins," *Nat Methods*, vol. 5, no. 8, pp. 683–685, Aug. 2008, doi: 10.1038/nmeth.1235.

[30] H. Tsutsui *et al.*, "Improved detection of electrical activity with a voltage probe based on a voltage‐sensing phosphatase," *J Physiol*, vol. 591, no. 18, pp. 4427–4437, Sep. 2013, doi: 10.1113/jphysiol.2013.257048.

[31] Y. Bando, C. Grimm, V. H. Cornejo, and R. Yuste, "Genetic voltage indicators," *BMC Biol*, vol. 17, no. 1, p. 71, Dec. 2019, doi: 10.1186/s12915-019-0682-0.

[32] J. J. Jun *et al.*, "Fully integrated silicon probes for high-density recording of neural activity," *Nature*, vol. 551, no. 7679, pp. 232–236, Nov. 2017, doi: 10.1038/nature24636.

[33] D. H. Hubel and T. N. Wiesel, "Receptive fields of single neurones in the cat's striate cortex," *J Physiol*, vol. 148, no. 3, pp. 574–591, Oct. 1959, doi: 10.1113/jphysiol.1959.sp006308.

[34] M. E. J. Obien, K. Deligkaris, T. Bullmann, D. J. Bakkum, and U. Frey,

"Revealing neuronal function through microelectrode array recordings," *Front Neurosci*, vol. 8, Jan. 2015, doi: 10.3389/fnins.2014.00423.

[35] X. Xu *et al.*, "Multi-sized microelectrode array coupled with micro-electroporation for effective recording of intracellular action potential," *Microsyst Nanoeng*, vol. 11, no. 1, p. 85, May 2025, doi: 10.1038/s41378-025-00887-6.

[36] O. P. Hamill, A. Marty, E. Neher, B. Sakmann, and F. J. Sigworth, "Improved patch-clamp techniques for high-resolution current recording from cells and cell-free membrane patches," *Pflugers Arch*, vol. 391, no. 2, pp. 85–100, Aug. 1981, doi: 10.1007/BF00656997.

[37] A. Robert. Martin, D. A. . Brown, M. E. . Diamond, Antonino. Cattaneo, F. Rafael. Fernández de Miguel, and J. G. . Nicholls, *From neuron to brain*. Oxford University Press, 2021.

[38] K. P. Harris and J. T. Littleton, "Transmission, Development, and Plasticity of Synapses," *Genetics*, vol. 201, no. 2, pp. 345–375, Oct. 2015, doi: 10.1534/genetics.115.176529.

[39] R. P. Kommaddi, R. Gowaikar, H. P A, L. Diwakar, K. Singh, and A. Mondal, "Akt activation ameliorates deficits in hippocampal-dependent memory and activity-

dependent synaptic protein synthesis in an Alzheimer's disease mouse model," *Journal of Biological Chemistry*, vol. 300, no. 2, p. 105619, Feb. 2024, doi: 10.1016/j.jbc.2023.105619.

[40] R. Anjum, V. R. J. Clarke, Y. Nagasawa, H. Murakoshi, and S. Paradis, "Rem2 interacts with CaMKII at synapses and restricts long-term potentiation in hippocampus," Mar. 12, 2024. doi: 10.1101/2024.03.11.584540.

[41] C. Montani, L. Gritti, S. Beretta, C. Verpelli, and C. Sala, "The Synaptic and Neuronal Functions of the X‐Linked Intellectual Disability Protein Interleukin‐1 Receptor Accessory Protein Like 1 (IL1RAPL1)," *Dev Neurobiol*, vol. 79, no. 1, pp. 85–95, Jan. 2019, doi: 10.1002/dneu.22657.

[42] Z. Yao *et al.*, "A high-resolution transcriptomic and spatial atlas of cell types in the whole mouse brain," *Nature*, vol. 624, no. 7991, pp. 317–332, Dec. 2023, doi: 10.1038/s41586-023-06812-z.

[43] M. D. Serruya *et al.*, "Engineered Axonal Tracts as 'Living Electrodes' for Synaptic‐Based Modulation of Neural Circuitry," *Adv Funct Mater*, vol. 28, no. 12, Mar. 2018, doi: 10.1002/adfm.201701183.

[44] K. Suzuki *et al.*, "A synthetic synaptic organizer protein restores glutamatergic

neuronal circuits," *Science (1979)*, vol. 369, no. 6507, Aug. 2020, doi: 10.1126/science.abb4853.

[45] K. Sekine, W. Haga, S. Kim, M. Imayasu, T. Yoshida, and H. Tsutsui, "Neuron-microelectrode junction induced by an engineered synapse organizer," *Biochem Biophys Res Commun*, vol. 712–713, p. 149935, Jun. 2024, doi: 10.1016/j.bbrc.2024.149935.

[46] W. Haga, K. Sekine, Sm. A. Hamid, M. Imayasu, T. Yoshida, and H. Tsutsui, "Development of artificial synapse organizers liganded with a peptide tag for molecularly inducible neuron-microelectrode interface," *Biochem Biophys Res Commun*, vol. 699, p. 149563, Mar. 2024, doi: 10.1016/j.bbrc.2024.149563.

[47] A. Abdi Ghavidel, V. Jajarmi, M. Bandehpour, and B. Kazemi, "Polycistronic Expression of Multi-Subunit Complexes in the Eukaryotic Environment: A Narrative Review.," *Iran J Parasitol*, vol. 17, no. 3, pp. 286–295, 2022, doi: 10.18502/ijpa.v17i3.10618.

[48] P. J. Shilling, K. Mirzadeh, A. J. Cumming, M. Widesheim, Z. Köck, and D. O. Daley, "Improved designs for pET expression plasmids increase protein production yield in Escherichia coli," *Commun Biol*, vol. 3, no. 1, p. 214, May

2020, doi: 10.1038/s42003-020-0939-8.

[49] D. M. Czajkowsky, J. Hu, Z. Shao, and R. J. Pleass, "Fc - fusion proteins: new developments and future perspectives," *EMBO Mol Med*, vol. 4, no. 10, pp. 1015–1028, Oct. 2012, doi: 10.1002/emmm.201201379.

[50] C. A. Combs, "Fluorescence Microscopy: A Concise Guide to Current Imaging Methods," *Curr Protoc Neurosci*, vol. 50, no. 1, Jan. 2010, doi: 10.1002/0471142301.ns0201s50.

[51] S. S. SHAPIRO and M. B. WILK, "An analysis of variance test for normality (complete samples)," *Biometrika*, vol. 52, no. 3–4, pp. 591–611, Dec. 1965, doi: 10.1093/biomet/52.3-4.591.

[52] W. H. Kruskal and W. A. Wallis, "Use of Ranks in One-Criterion Variance Analysis," *J Am Stat Assoc*, vol. 47, no. 260, pp. 583–621, Dec. 1952, doi: 10.1080/01621459.1952.10483441.

[53] A. Dinno, "Nonparametric Pairwise Multiple Comparisons in Independent Groups using Dunn's Test," *The Stata Journal: Promoting communications on statistics and Stata*, vol. 15, no. 1, pp. 292–300, Apr. 2015, doi: 10.1177/1536867X1501500117.

[54] D. Araç *et al.*, "Structures of Neuroligin-1 and the Neuroligin-1/Neurexin-1 β Complex Reveal Specific Protein-Protein and Protein-Ca2+ Interactions," *Neuron*, vol. 56, no. 6, pp. 992–1003, Dec. 2007, doi: 10.1016/j.neuron.2007.12.002.

[55] T. Yoshida *et al.*, "IL-1 Receptor Accessory Protein-Like 1 Associated with Mental Retardation and Autism Mediates Synapse Formation by *Trans* -Synaptic Interaction with Protein Tyrosine Phosphatase δ," *The Journal of Neuroscience*, vol. 31, no. 38, pp. 13485–13499, Sep. 2011, doi: 10.1523/JNEUROSCI.2136-11.2011.

[56] W. Haga, K. Sekine, Sm. A. Hamid, M. Imayasu, T. Yoshida, and H. Tsutsui, "Development of artificial synapse organizers liganded with a peptide tag for molecularly inducible neuron-microelectrode interface," *Biochem Biophys Res Commun*, vol. 699, p. 149563, Mar. 2024, doi: 10.1016/j.bbrc.2024.149563.

[57] S. R. Heidemann, M. Reynolds, K. Ngo, and P. Lamoureux, "The Culture of Chick Forebrain Neurons," 2003, pp. 51–65. doi: 10.1016/S0091-679X(03)01004-5.

[58] S. L. Shipman and R. A. Nicoll, "Dimerization of postsynaptic neuroligin drives

synaptic assembly via transsynaptic clustering of neurexin," *Proceedings of the National Academy of Sciences*, vol. 109, no. 47, pp. 19432–19437, Nov. 2012, doi: 10.1073/pnas.1217633109.

[59] S. Kim, M. Imayasu, T. Yoshida, and H. Tsutsui, "Formation of neuron-microelectrode junction mediated by a synapse organizer," *Applied Physics Express*, vol. 16, no. 5, p. 057003, May 2023, doi: 10.35848/1882-0786/acd166.

[60] Nan Xinyu, "Exploration of a molecular tool for neuronal circuit editing ," Japan Advanced Institute of Science and Technology, 2023.

[61] D. G. Grier, "A revolution in optical manipulation," *Nature*, vol. 424, no. 6950, pp. 810–816, Aug. 2003, doi: 10.1038/nature01935.

[62] M. A. L. Nicolelis, "Actions from thoughts," *Nature*, vol. 409, no. 6818, pp. 403–407, Jan. 2001, doi: 10.1038/35053191.

Acknowledgement

First and foremost, I would like to extend my sincere gratitude to my mentor Professor Dr. Hidekazu Tsutsui, for his immense patience and wisdom support throughout my seven years of study in Jaist. His meticulous guidance and creative insights have been invaluable throughout my academic journey. Whenever I encountered confusion or felt lost in my research, Professor Tsutsui always provided the most direct and clear direction, bolstering my confidence and perseverance in both my research and learning endeavors. I am deeply grateful for his unwavering support.

I sincerely appreciate Dr. Yuichi Hiratsuka's generous support and advice as an advisor for Minor research and for his technical assistance. I am also immensely thankful to Ms. Mieko Imayasu from the research institute for her experimental support and academic advice. Her enthusiastic assistance and dedication have been crucial to the success of this study.

I would like to express my appreciation to all my seniors and friends, especially Hamid, Samyoung Kim, Kosuke Sekine, Wataru Haga, for their encouragement and companionship during my time at JAIST. Their support has been a constant source of motivation and joy.

Lastly, I would like to express my deepest gratitude to my father and mother, who have been the steadfast supporters of everything I have achieved.